

## **INTRODUCTION**

### **1.1 GENERAL**

The word ‘photonics’ originated from a Greek word ‘photos’ which means light. This term came into sight in the late 1960s to depict a research field whose objective was to utilize light to perform functions that customarily fell inside the standard domain of electronics, such as telecommunications, information handling, etc. The era of photonics began with the invention of laser in 1960, followed by laser diode in the 1970s. Optical fibers and erbium doped fiber amplifier (EDFA) were also invented subsequently. These innovations shaped the reason for the telecommunications reformation of the late twentieth century and contributed towards the foundation of the Internet. In spite of the fact that the term photonics was minted earlier, it came into regular use in the 1980s as fiber-optic information transmission was embraced by telecommunications system operators. Around then, the term was utilized generally at Bell Laboratories. Its utilization was affirmed when the IEEE Lasers and Electro-Optics Society built up a chronicled journal named Photonics Technology Letters towards the finish of 1980s. Apart of telecommunication, photonics covers a tremendous scope of science and innovation applications, which include laser based production, organic and inorganic substance detection, therapeutic diagnostics and treatment, display innovation, and optical computing. Photonics is associated with quantum optics, optomechanics, electro-optics, optoelectronics and quantum electronics. Nonetheless, every domain has somewhat unique implication by logical and government bodies and in the commercial area.

Applications of photonics are omnipresent. Comprised are all fields from everyday life to the most evolved technologies, e.g. light detection, telecommunications, information processing, photonic computing, lighting, metrology, spectroscopy, holography, medicine (surgery, vision correction, endoscopy, health monitoring), military technology, laser material processing, visual art, bio-photonics, agriculture, and robotics. Light sources utilized as a part of photonics are generally far more advanced than the conventional light bulbs. Photonics ordinarily employs semiconductor light sources like light-emitting diodes (LEDs), super-luminescent diodes, and lasers. Talking about the transmission media, light can be communicated via any see-through channel. Glass fiber or plastic optical fiber can be utilized to transfer the light along a suitable direction. Depending upon the bit rate and the type of modulation scheme applied at the input, optical fibers are able to carry optical signals for hundreds of kilometers without any amplification. An exceptionally advanced exploration field inside photonics is the examination and creation of unique structures and materials with designed optical properties. These include photonic crystals, photonic crystal fibers and meta-materials. Optical fibers are preferred transmission media over metal wires because they provide low loss to signals travelling along them, also fibers are immune to electromagnetic interference, which metal wire is not. Other advantages of fiber over metal wires are large bandwidth, electrical insulation, low material cost, and security of information. Fibers which support a number of proliferation paths or transverse modes are called multi-mode fibers (MMF), whereas those that support only a single mode are called single-mode fibers (SMF). Optical fibers can be utilized as sensors to calculate strain, temperature, pressure and other parameters by the modification of certain property of light in the fiber such as intensity, phase, polarization, wavelength, or transit time. Optical fibers have a prominent application in medical field. Where bright light is needed to illuminate a

target and approach path of target is narrow, optical fibers are used as light guides. Optical fibers are generally made of silica and plastic material, for advanced applications other materials such as germanium is also been included in limited quantities to manufacture optical fibers.

Photonics crystals are the periodic arrangement of a medium in one, two or three dimensions to form a structure which is able to show specific applications in context of light. They are basically built of semi-conductor materials with thicknesses ranging from micrometer to nanometer [1, 2]. Circuits based on photonic crystals have the potential to control the flow of light, just as in the case of solid state circuits which have the ability to manipulate motion of electronic current. As the research on photonic crystals progressed, people started to find more and more number of applications based on them. There is a periodic variation in refractive index and distance both, between two constituent units in a photonic crystal. Due to this variation, a particular frequency or a range of frequencies can be allowed to pass through a photonic crystal or can be stopped by the photonic crystal. An important term related to photonic crystals is their band-gap, which means a range of frequencies that are completely blocked by the photonic crystal to pass through them [3]. 1-D, 2-D and 3-D photonic crystal structures in simple forms are shown in Figure 1.1 (a), (b) and (c) respectively [4].

PC structures exhibiting photonic band-gap (PBG) property were first studied by Yablonovitch [5] and John [6] in the late 1980s. After that, the quantity of research papers related to PCs started growing rapidly. Challenges in creation of PC structures at optical scales, led to early studies as either hypothetical or in the microwave region, where the structural dimensions are in the nanometer scale.

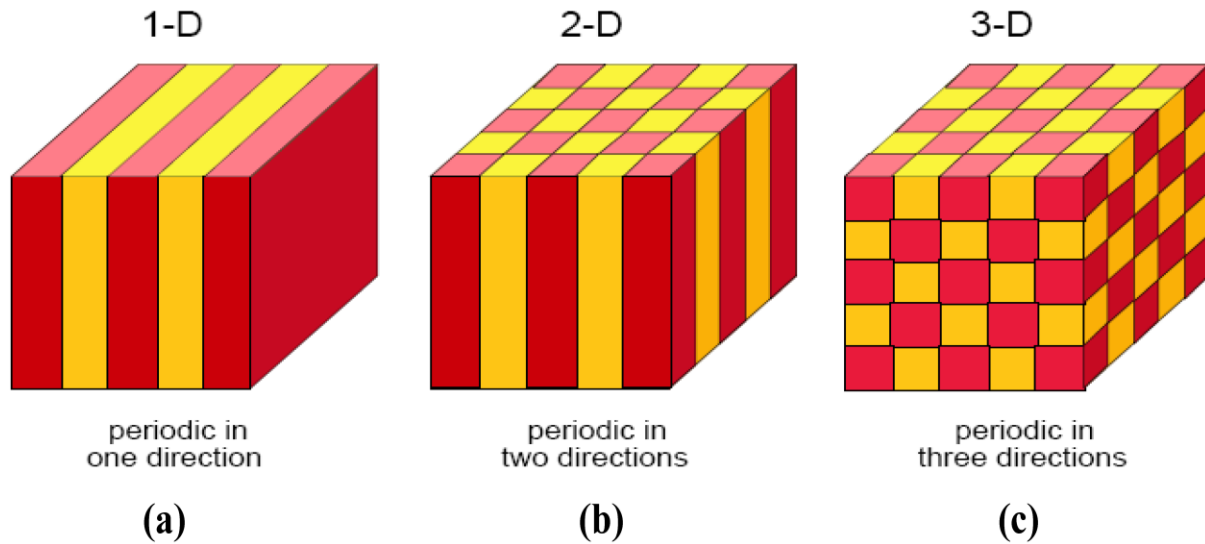


**Figure 1.1** The geometrical shape of (a) 1DPCs, (b) 2DPCs and (c) 3DPCs where the different colors represent material with different dielectric constants

## 1.2 NUMERICAL ANALYSIS

There are a quite number of techniques accessible to examine the dispersion phenomena and transmission scope of PCs like beam propagation method (BPM) [7], multi-pole method (MPM) [8], finite element method (FEM) [9], transfer matrix method (TMM) [10], plane wave expansion (PWE) [11] and finite difference time domain method (FDTD) [12] etc. FEM and FDTD are much sought out methods amongst all as FEM is easier to implement whereas FDTD is more accurate. FDTD can be applied to programming of 2-D or 3-D PC structure codes with equal power. The TMM is suitable to solve 1-D PC structure as it reduces the complexity of a linearly layered arrangement. The PWE technique is utilized to determine the PBG and proliferation methods of the PC structure especially in two-dimensions.

### **1.3 APPLICATIONS OF 2-D PCS**

A wide range of optical devices based on the involvement of 2-D PCs, have been practically manufactured and further research is going on to make them more advance [13]. 2-D PC structures can have naturally or be given hexagonal, square, triangular etc. type of symmetry. When a single rod of semiconductor or a number of rods from the PC structure are eliminated, then a defect is generated. This defect provides a wave-guiding phenomenon in the PC structure. Light can also be trapped into a PC structure by formation of a resonant cavity. Optical filters, wavelength multiplexers and de-multiplexers, power couplers etc. optical devices can be built based on 2-D PCs [14]. Photonic crystal ring resonator (PCRR) is an important application of 2-D PCs, in which a central ring cavity is formed by removing specific quantity of semiconductor rods from central region. Another significant application of PC is in the fabrication of a special type of optical fiber known as, photonic crystal fiber (PCF).

### **1.4 PHOTONIC CRYSTAL FIBER**

Photonic crystal fibers (PCF) have proved to be advantageous in many respects than the conventional optical fibers. PCF structure contains an array of air holes as part of its cladding that distinguishes it from the conventional optical fibers which have only a core and cladding or a combined core and cladding in case of multi-mode graded index fiber [15]. There are two types of PCF based on light guidance inside the core, one works on effective index method and the other on photonic band-gap (PBG) effect. The PCF with effective index guiding phenomena consists of solid core while the other type of PCF based on PBG consists of hollow core. In the effective index based guidance of light the mechanism is similar as compared to the guidance of light in conventional single-mode

optical fibers. In this case, there is a modified total internal reflection (M-TIR) in the PCF since the refractive index of cladding keeps changing with the wavelength applied. The core region has a higher refractive index as compared to the composite refractive index of cladding in this type of PCF [16, 17]. Usually pure silica with refractive index 1.45 is used to make the core of these PCF's but other glasses or materials of higher refractive index could also be used to make the core for proper light guidance. These kinds of PCF's show unique properties such as atypical dispersion exhibition over visible and near infra-red range, transportation of ultra-short pulses and with-standing a wide range of wavelengths [18]. Considering the other type of PCF which is based on PBG guidance mechanism, the core has a lower refractive index as compared to the effective refractive index of surrounding cladding. There is a PBG effect in the two dimensional photonic crystal cladding which does not allow light in certain wavelength range to propagate through it [19]. This PBG effect can also be seen in nature, for example the beautiful color combination visible on peacock feathers and butterfly wings is a result of the same. If light is guided into the air core of PBG guidance based PCF, the PCF can provide many favorable applications such as low loss guidance and high-power beam delivery without any damages to the fiber. These types of PCF are almost insensitive to bending even for very sharp bends subjected to the fiber. Filling the hollow air core with liquids or gases can make these fibers to be used as sensors. A schematic cross-section of a circular hole hexagonal PCF is shown in Figure 1.2. In this figure,  $\Lambda$  denotes pitch of the fiber, which is the distance between centers of two consecutive air holes whereas 'd' stands for the diameter of a single air hole.

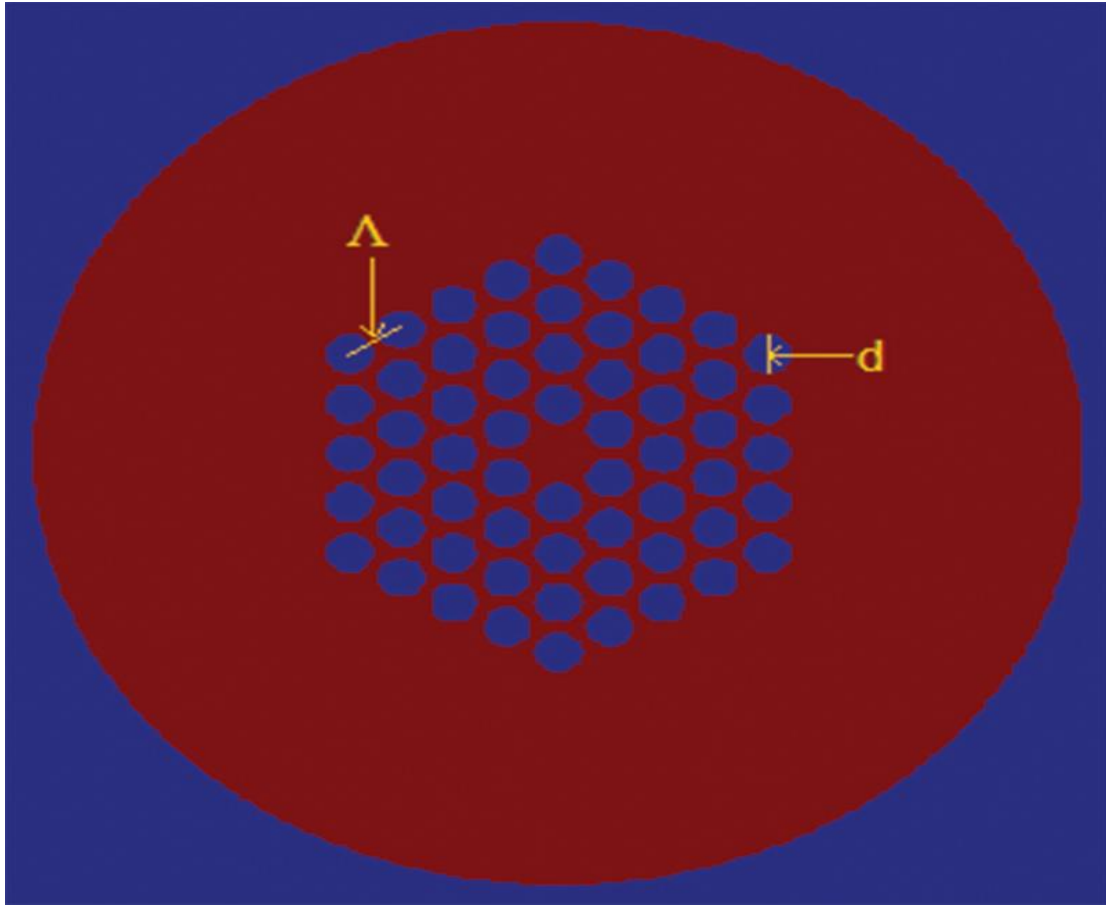


**Figure 1.2** Hexagonal lattice photonic crystal fiber with 4 rings of air holes.

A lot of research has been done on the optimization of the structure of PCF for improved applications [20-24]. High negative dispersion has been achieved in PCF by modifying the structural parameters [25]. Mainly we can control two parameters of PCF which are air-hole size in the cladding region and the distance between those air holes called pitch. Besides hexagonal and triangular lattice, a PCF structure can also be fabricated based on square or rectangular lattice configuration in the cladding [26, 27]. Talking about the holes in the cladding, they can be fabricated with different types of shapes which include circular [28], elliptical [29], square [30] or rectangular [31]. A lot of work has been

done on hybrid structure PCF's which contain a combination of the above mentioned lattice and hole types [32-34].

PCF can show exceptional dispersion properties as compared to standard optical fibers. In addition to dispersion, other properties of PCF are also studied and optimized such as birefringence, confinement loss, effective area and normalized frequency [35-37]. Initially PCF structure was proposed, based on hexagonal lattice as part of its cladding containing air-holes. A. Bjarklev et al. in 1998 were the first to work on the dispersion properties of PCF [38]. An effective index model [39] was used to simulate a hexagonal type PCF. They compared the spot-sizes of PCF with standard silica fiber and observed that the PCF has quite poor wavelength sensitivity with respect to standard fiber. The air filling fraction was a limiter to the dispersion values of PCF. If the air filling fraction is increased, the dispersion of PCF also gets increased and contains a higher portion of the waveguide dispersion. Flattened and negative dispersion is seen by optimization of the structural parameters of the PCF especially distance between two air holes, known as pitch.

The important parameters related to PCF which can be calculated are:

#### **1.4.1 Chromatic Dispersion**

Chromatic dispersion is a major factor which causes pulse broadening in optical fibers. It is composed of material and waveguide dispersion [40, 41]. The chromatic dispersion (D) of PCF is given by the equation:

$$D = D_m + D_w \quad (1.1)$$

Here,  $D_m$  stands for material dispersion and  $D_w$  is the waveguide dispersion. Interaction of different wavelengths with ions, molecules or electrons in a material generates material dispersion. While waveguide dispersion depends on the structure of the PCF specifically the size, arrangement of air-holes in the cladding and the refractive index contrast between that of core and cladding. The equation for material dispersion ( $D_m$ ) is given by -

$$D_m = - \frac{\lambda}{c} \frac{\partial^2 (n_m)}{\partial \lambda^2} \quad (1.2)$$

And that for waveguide dispersion ( $D_w$ ) is given by -

$$D_w = - \frac{\lambda}{c} \frac{\partial^2 [\text{Re}(n_{\text{eff}})]}{\partial \lambda^2} \quad (1.3)$$

In the Equations (1.2) and (1.3),  $\lambda$  is the wavelength of light used,  $n_m$  is the refractive index of material,  $\text{Re}(n_{\text{eff}})$  is the real part of  $n_{\text{eff}}$  where  $n_{\text{eff}}$  is the effective refractive index and  $c$  is the velocity of light. The material dispersion can be calculated by using the Sellmeir equation [42].

### 1.4.2 Effective Area

The effective area for a PCF structure can be evaluated by using the equation [43]:

$$A_{\text{eff}} = \frac{(\iint |E|^2 dx dy)^2}{\iint |E|^4 dx dy} \quad (1.4)$$

In the above equation  $E$  is the electric field applied to the structure at the core and  $dx$ ,  $dy$  are the transverse components of surface area of the input end of PCF. Effective area is a measure of the area covered by the fundamental mode propagating in the fiber and it keeps increasing with the increase in the operating wavelength. If effective area is small, it provides high values of non-linear coefficient ( $\gamma$ ) as  $\gamma$  is inversely proportional to  $A_{\text{eff}}$ . The

high values of  $\gamma$  make this fiber suitable to be used in non-linear optics [44], super continuum generation [45] and soliton pulse propagation [46]. Also the fiber becomes more insensitive to bending.

### 1.4.3 Normalized frequency

The equation to determine normalized frequency ( $V_{\text{eff}}$ ) of any PCF [47] is given as :

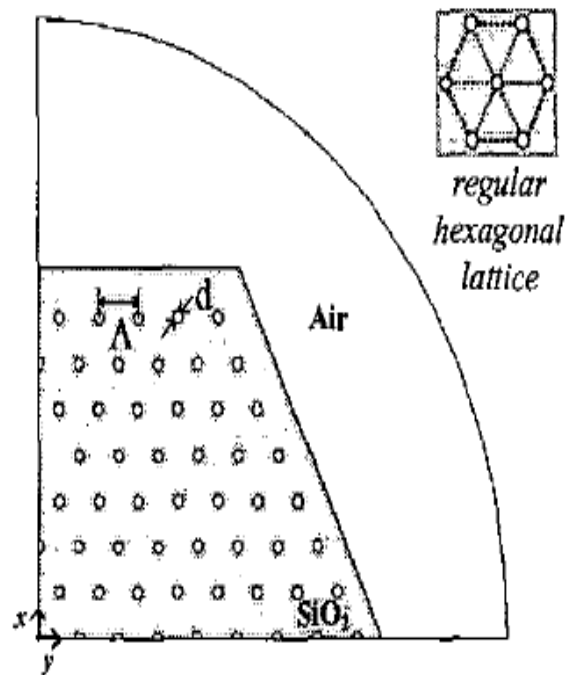
$$V_{\text{eff}} = \frac{2\pi}{\lambda} \Lambda (n_{\text{co}}^2 - n_{\text{eff}}^2)^{1/2} \quad (1.5)$$

$\Lambda$  (pitch) stands for the distance between the centers of two consecutive air-holes while  $n_{\text{co}}$  indicates the refractive index of core of the PCF. The type of mode propagation in the PCF can be decided on the basis of the values of  $V_{\text{eff}}$  obtained. A PCF has the ability to operate in multimode state in addition to single mode during the propagation of an electromagnetic wave.

In 1999, A. Ferrando et al. did a full vector analysis of photonic crystal fiber in their work [48]. They have used a biorthogonal modal method [49] reported in one of their earlier work, for simulation of PCF. A hexagonal lattice structure PCF was taken for computations with a central defect in the core. The hole radius was fixed at 0.3  $\mu\text{m}$  and the pitch of the lattice as 2.3  $\mu\text{m}$ . The dispersion results calculated theoretically are in agreement with those of the experimental at 632.8 nm wavelength. The PCF remains single-moded in a wide wavelength range viz. 337 to 1550 nm. In the same year, A. Ferrando et al. published another work related to PCFs optimization of chromatic dispersion [50]. Flattened dispersion and nearly zero dispersion have been achieved in the wavelength range 300-1600 nm. Relation of structural parameters of PCF viz. pitch and radius of air holes with the dispersion characteristics is established.

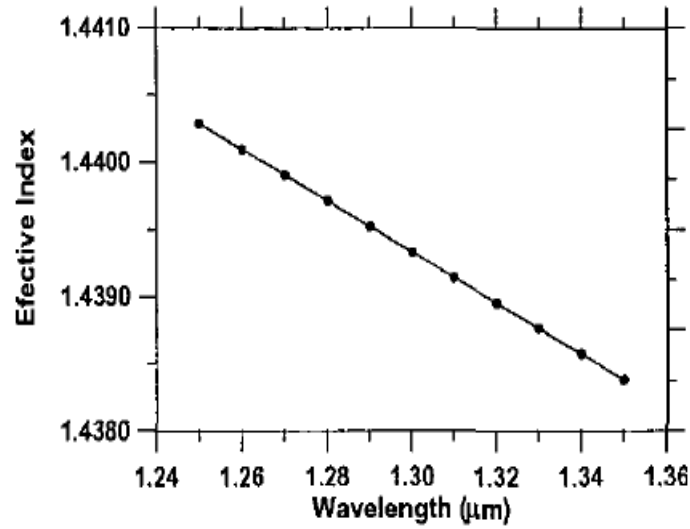
There are a number of methods to theoretically investigate the working of PCFs. A finite element method [51] was the basis of simulation of PCFs in the earlier times as it is easier to implement and time saving as compared to other methods. M. A. R. Franco et al. in their work in 2001 studied effective index, dispersion and effective area parameters of PCF using a scalar effective index method [52]. They started with a Helmholtz equation for FEM modelling and solved it by converting it into a matrix form. At first, effective index values of PCF are computed and using them chromatic dispersion is determined by using the Equation 1.1. Also, effective area has been calculated for the PCF using Equation 1.4.

FEM model is applied to a quarter of the cross-section of PCF, containing hexagonal lattice of air-holes as part of cladding as shown in Figure 1.3.



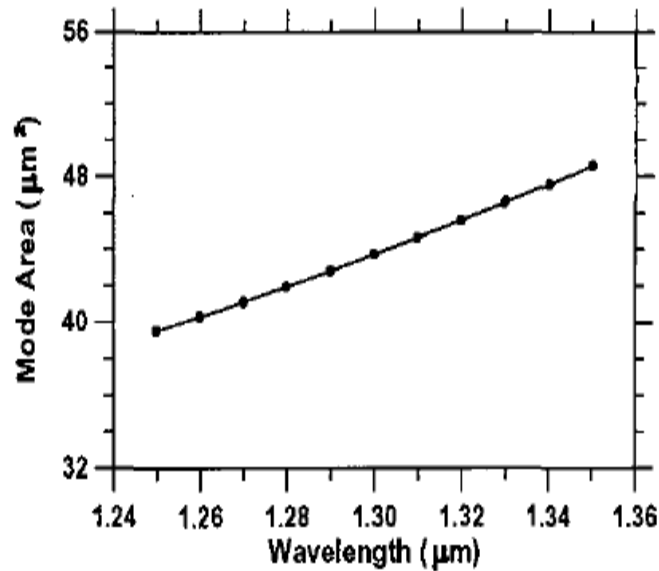
**Figure 1.3** A quarter of the cross-section of PCF containing hexagonal lattice of air holes.

A linear relation between effective index values and wavelength has been achieved for the PCF, as shown in Figure 1.4.



**Figure 1.4** Effective refractive index of PCF as a function of wavelength.

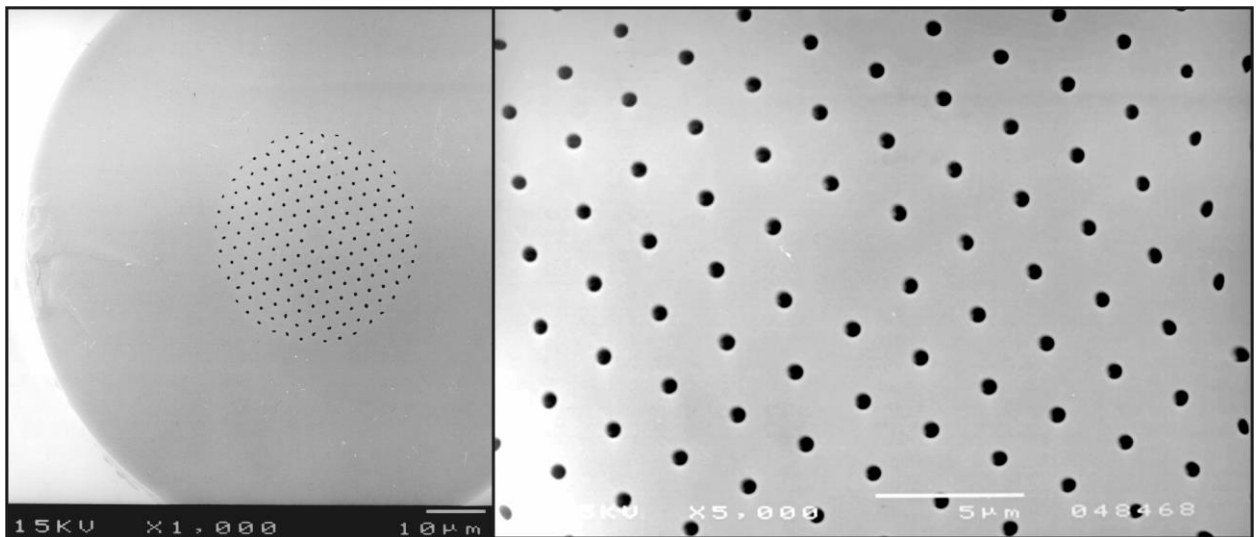
The effective area of PCF calculated, increases with the increase in wavelength, as plotted in Figure 1.5. This happens because the larger wavelength field spreads more into the cladding air-hole region in all directions, thus increasing the effective area covered by the field.



**Figure 1.5** Effective area of PCF as a function of wavelength.

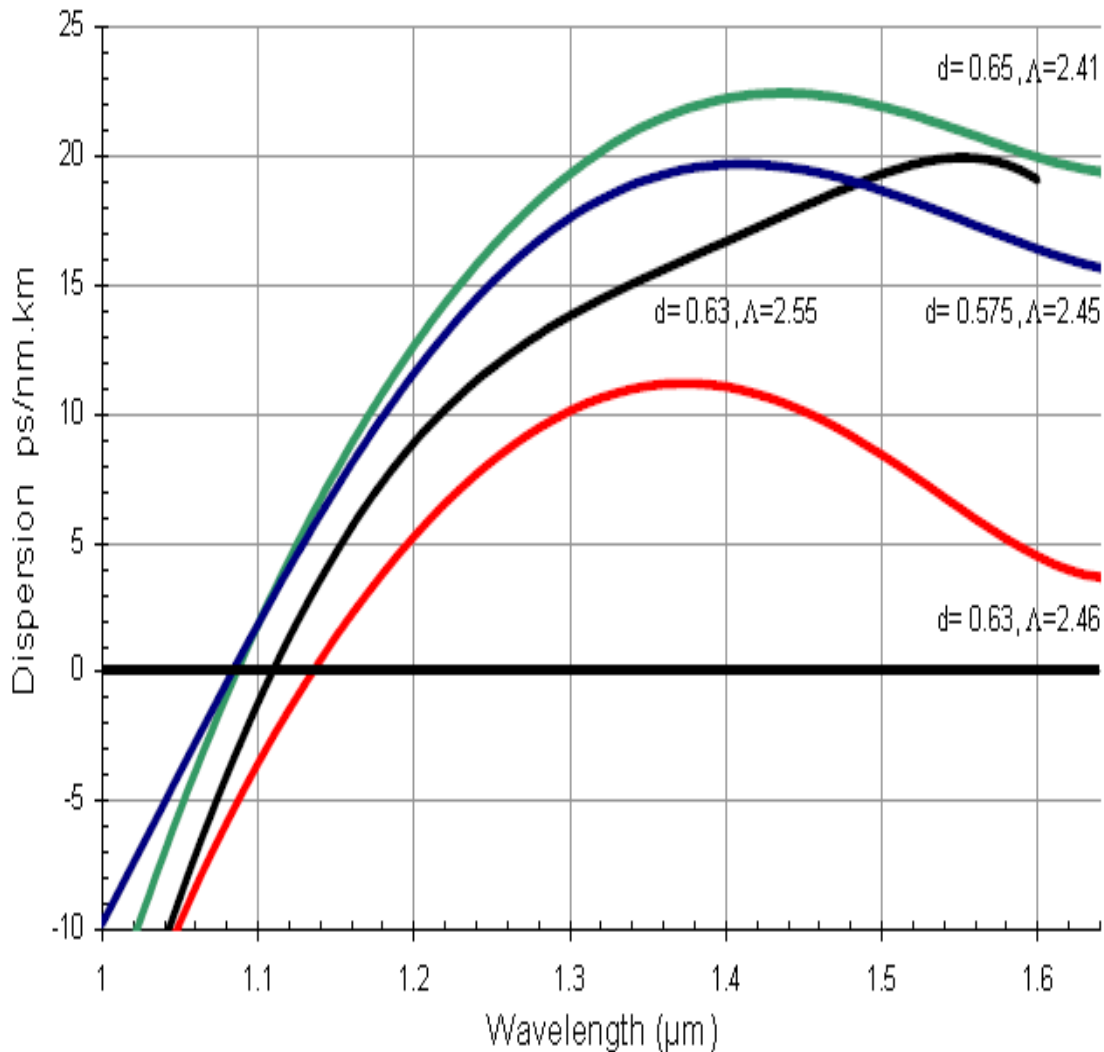
In all, they have successfully computed the main parameters of PCF with the help of a finite-element model in their work.

Demonstration of ultra-flattened dispersion in photonic crystal fibers was studied by W.H. Reeves et al. in their work in 2002 [53]. They fabricated two micro-structured fibers showing dispersion of  $0 \pm 0.6$  ps/nm-km from 1.24  $\mu\text{m}$ -1.44  $\mu\text{m}$  wavelength and  $0 \pm 1.2$  ps/nm-km over 1  $\mu\text{m}$ -1.6  $\mu\text{m}$  wavelength. Precise control of air holes shape, size, pitch and core diameter in fibers is essential for demonstration of ultra-low dispersion. The first fiber they fabricated had a hole diameter,  $d = 0.63$   $\mu\text{m}$  and distance between two adjacent air holes, pitch as 2.64  $\mu\text{m}$ . In total, 186 air holes were embedded into the fiber and the dispersion was calculated experimentally by using a low coherence interferometric technique [54]. The electron micrograph of one of the fibers they fabricated is shown in Figure 1.6.



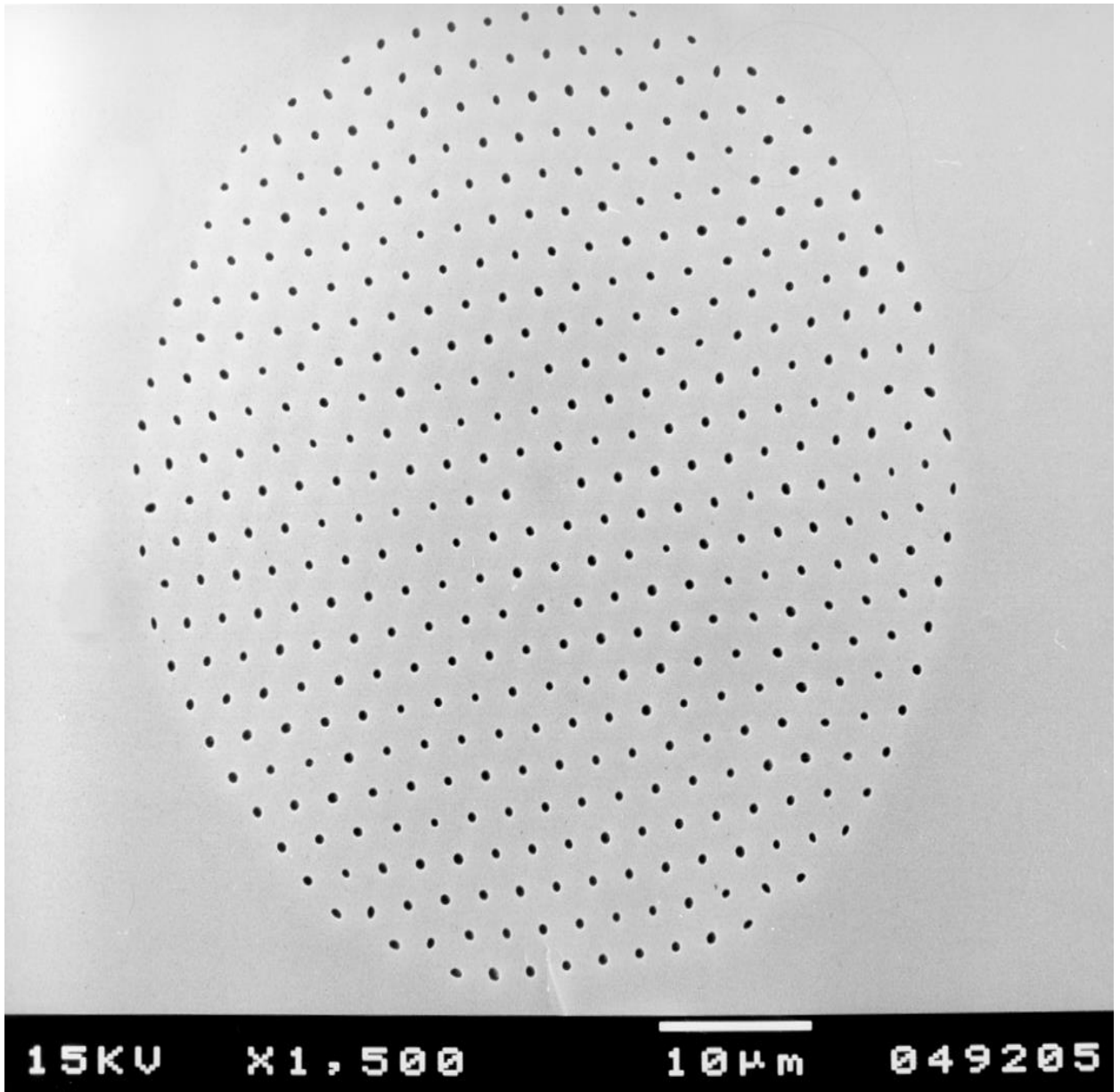
**Figure 1.6** A photonic crystal fiber with 7 periods in the cladding and with  $\Lambda = 2.5$   $\mu\text{m}$  and  $d = 0.5$   $\mu\text{m}$ .

Figure 1.7 shows the measured dispersion for a selection of PCFs with different values of hole diameter and pitches.



**Figure 1.7** Measured dispersion for a selection of 7 air-hole ring PCFs.

To overcome the gap in dispersion characteristics of experimental and modeled PCF, they made a new fiber with total of 455 air holes placed in 11 rings of cladding. Figure 1.8 shows an electron micrograph of this second PCF.



**Figure 1.8** Ultra-flattened dispersion photonic crystal fiber with 11 periods.  $\Lambda = 2.47\mu\text{m}$  and an average  $d$  of  $0.57\mu\text{m}$ .

They further took two 235 mm sections of the second type of fiber with different air hole diameter and pitch values and calculated dispersion characteristics as shown in Figure 1.9.

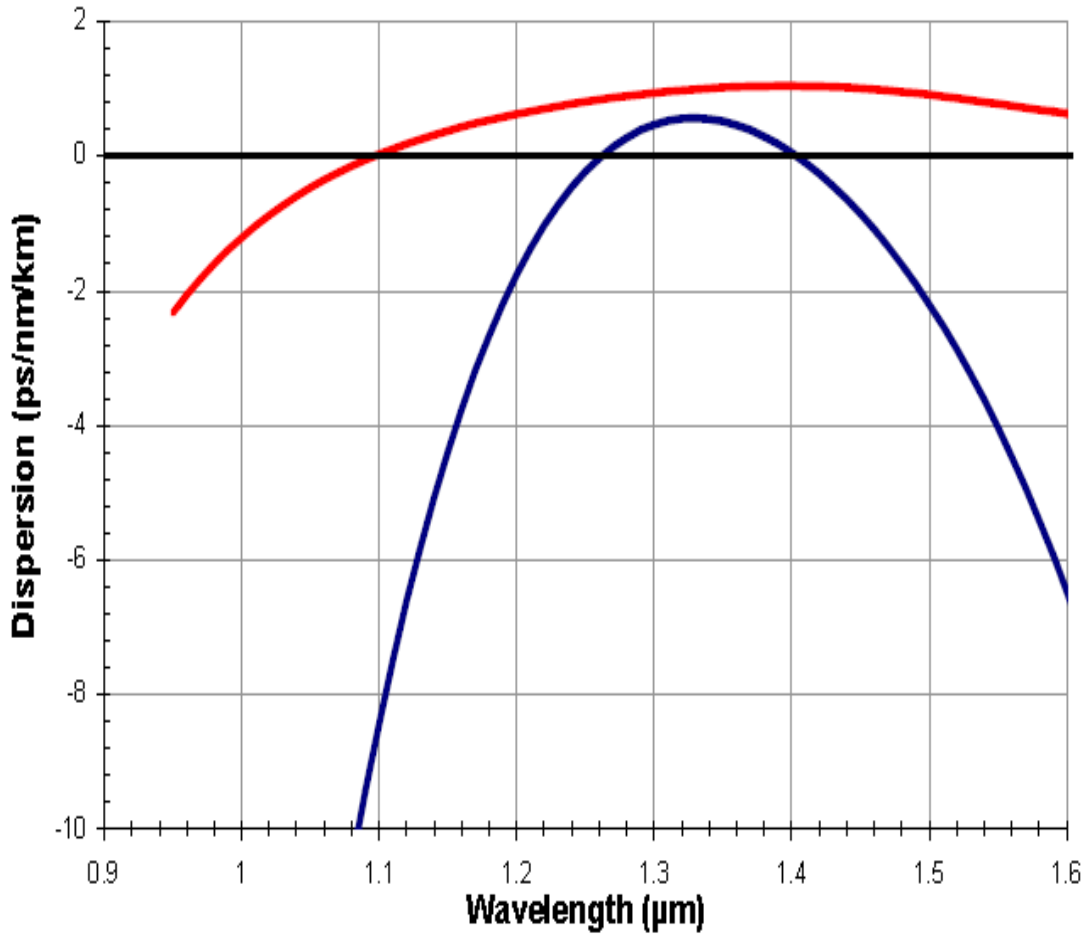


**Figure 1.9** Measured dispersion plots for ultra-flattened dispersion PCF. Red curve:  $d = 0.58$ ,  $\Lambda = 2.59$ , dark blue curve:  $d = 0.57$ ,  $\Lambda = 2.47$ .

PCFs or microstructured fibers can contain a number of lattice shapes as part of their cladding [55-57]. The guiding properties of PCF having square lattice of air-holes was first studied by A. H. Bouk et al. in 2004 [58]. An experimental preform of square lattice PCF was already fabricated before they started their theoretical work [59]. The diameter of air-holes and pitch in the cross-section of fiber have been varied to optimize the results, Figure 1.10 shows the air-holes arranged in square configuration.

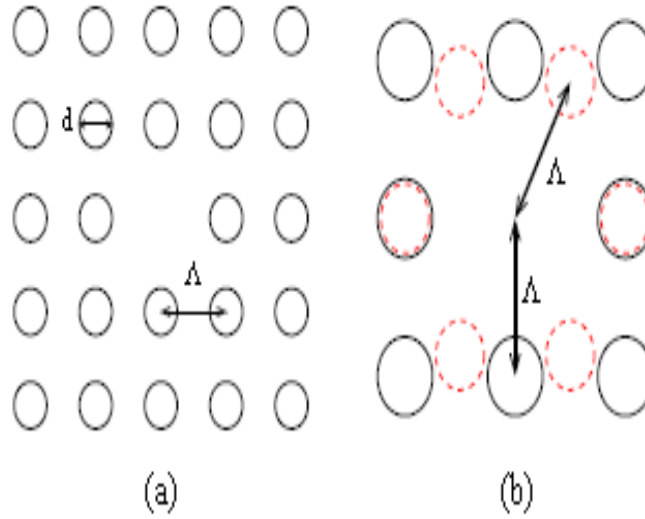


**Figure 1.10** (a) Cross-section of the square-lattice PCF. (b) Comparison of the air-hole positions in the first ring for square (dark line) and triangular (light line) lattices.

A full vectorial finite element method (FEM) has been applied to simulate the fiber [60]. Values of effective index are calculated using FEM approach in the wavelength range 1200 to 1600 nm and then using these values, dispersion parameters have been derived by applying simple finite-difference equations [61]. Perfectly matched layers [62] as boundary conditions along with FEM are used to take account of the leakage losses of PCF for small values of pitch. Simulations for different values of pitches and air hole dimensions have been done, in all the cases negative dispersion has been achieved. When the pitch ( $\Lambda$ ) is kept at the lowest i.e. equal to 1  $\mu\text{m}$ , the negative dispersion is visible in the C-band of communication, close to 1550 nm. The smallest amount of dispersion value at 1550 nm computed is  $-277$  ps/nm-km by keeping  $\Lambda=1$   $\mu\text{m}$  and ratio of pitch to diameter of air-hole ( $d/\Lambda$ ) equivalent to 0.6. The amount of dispersion increases with the increase in air-hole diameter, so for  $d/\Lambda \leq 0.7$  only, negative dispersion is observable. In case of triangular lattice PCFs as the pitch is increased, the effect of waveguide dispersion decreases, this

phenomenon is also confirmed for square-lattice PCFs. A comparison of the dispersion properties of five air-hole rings square and triangular lattice PCF has been done for different  $d/\Lambda$  and  $\Lambda$  values. A part of the comparison is shown in Figure 1.11, from which it can be observed that there is more negative dispersion and lower effective area for triangular lattice PCF at 1550 nm.

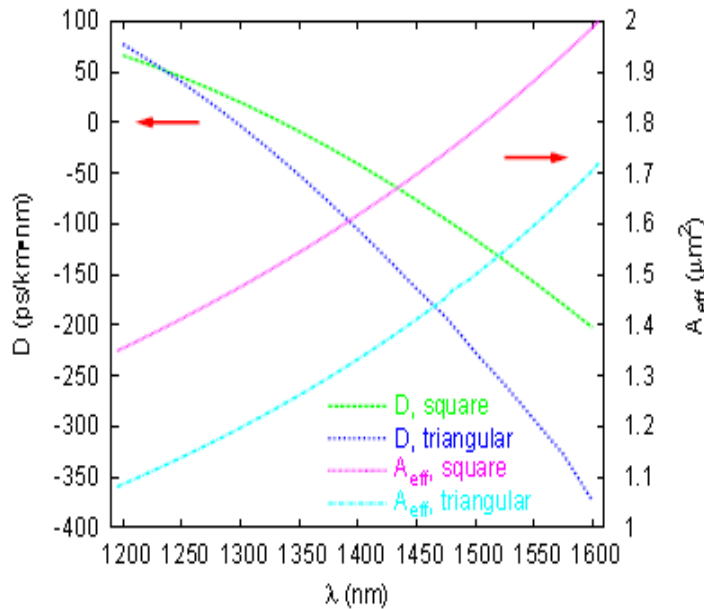


**Figure 1.11** Comparison of the dispersion parameter and the effective area values for the square lattice PCF and the triangular one with  $d/\Lambda = 0.9$  and  $\Lambda = 1 \mu\text{m}$ .

The dispersion slopes are not much affected by the variation of lattice geometry from triangular to square. Due to the maximum field confinement by the first air-hole ring, square-lattice PCFs are more useful in application as pig-tail fibers within integrated optical devices comprising a rectangular or a square cross-section.

In 2005, T. Matsui et al. presented a dispersion-flattened photonic crystal fiber with large effective area and low confinement loss [63]. They have proposed the design of a

novel dispersion flattened PCF (DF-PCF) and compared its dispersion characteristics with conventional PCF. The DF-PCF contains two cladding layers having different effective indices. A combination of air holes as defect is created into the central region of PCF as can be seen in Figure 1.12. The refractive index profiles of conventional as well as DF-PCF are also visible in the same figure.

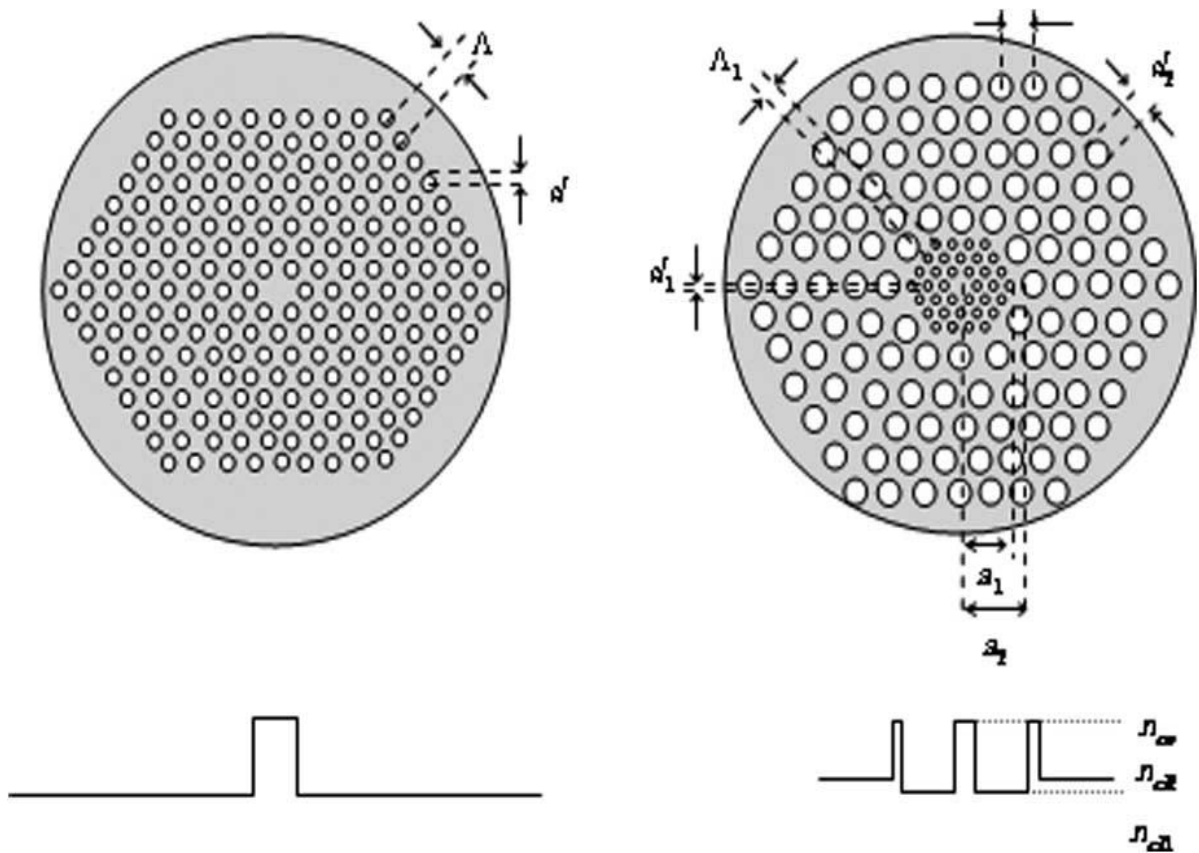


**Figure 1.12** Cross sections of PCFs and their effective-index profiles: (Left) Conventional PCF. (Right) DF-PCF.

Figure 1.13(a) shows the dispersion characteristics of the designed DF-PCF while Figure 1.13(b) shows the effective area and confinement loss of the DF-PCF. At the

communication wavelength 1550 nm, Figure 1.13(c) shows the fundamental mode-field distribution of the DF-PCF.

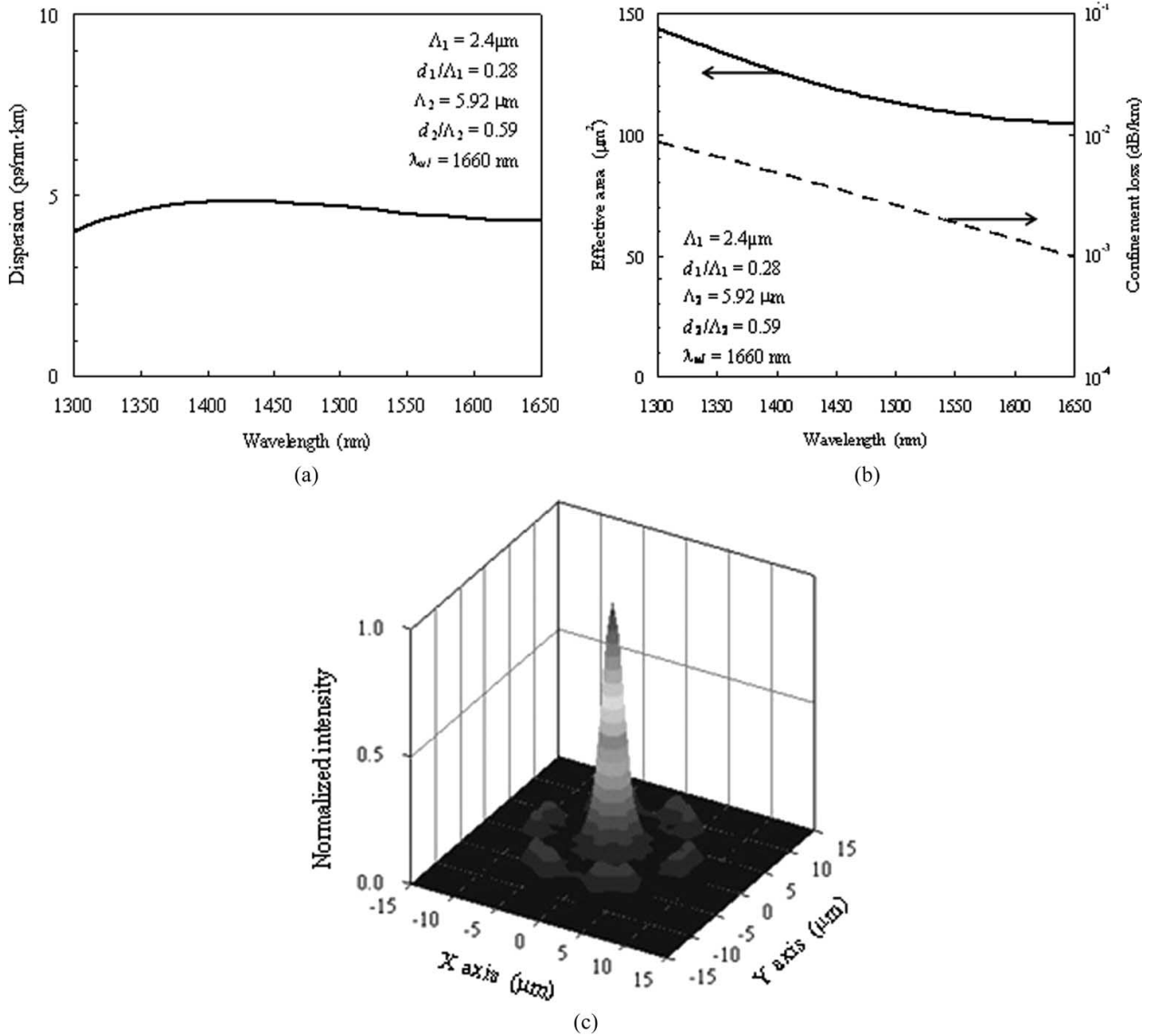


**Figure 1.13** Characteristics of the DF-PCF, where  $\Lambda_1 = 2.4 \mu\text{m}$ ,  $d_1/\Lambda_1 = 0.28$ ,  $R_a = 1.34$ , and  $R_n = -0.05\%$ . (a) Chromatic dispersion. (b) Effective area and confinement loss. (c) Mode-field distribution at a wavelength of 1550 nm.

Here,  $R_a$  corresponds to the width of the second core and  $R_n$  is the effective index difference between inner and outer cladding. Other parameters of the DF-PCF can be seen in Figure 1.12. In all, a dispersion- flattened photonic crystal fiber (DF-PCF) with a novel

structure consisting of two cladding layers that can provide ultra-flat chromatic dispersion, low confinement loss, and a large effective area has been proposed.

J. Wang et al. in 2007 presented the dispersion and polarization properties of elliptical air-hole-containing photonic crystal fibers [64]. Full-vectorial (PWE) method highly suitable for the examination of periodic arrangement has been applied to study the dispersion properties of triangular PCFs [65]. The modified form of PCF designed by them can be seen in Figure 1.14, it has circular air holes converted into elliptical air holes.

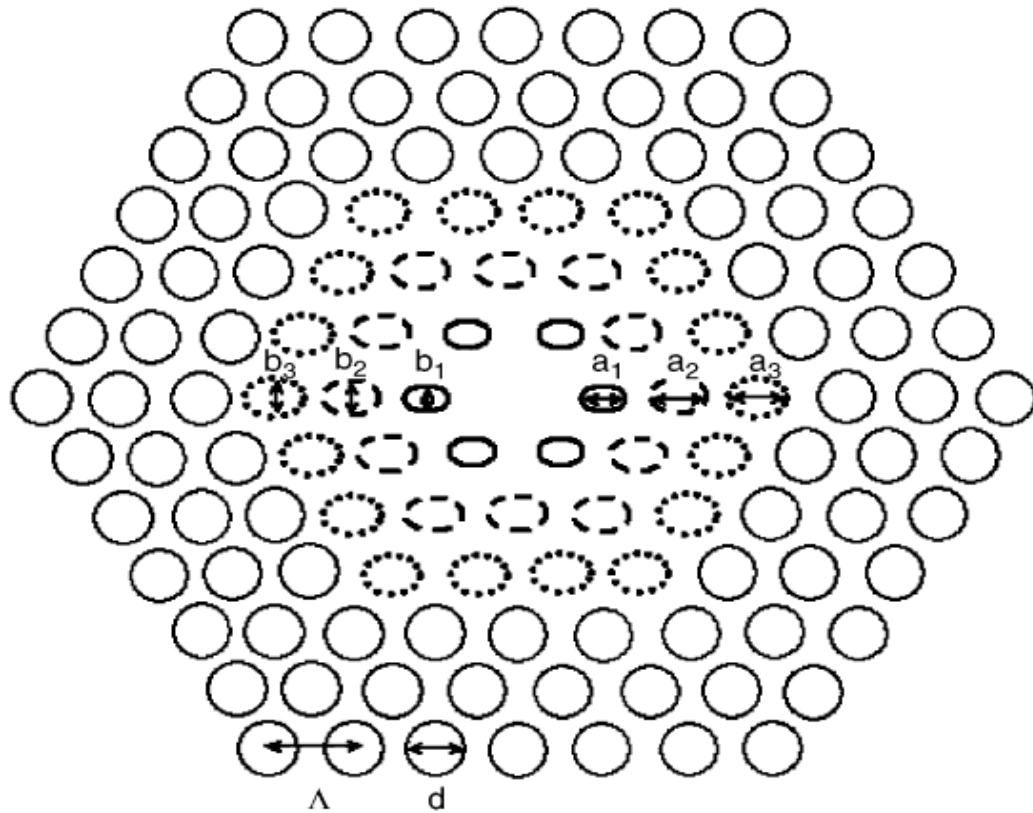


**Figure 1.14** PCF with three rings of elliptical air-holes. (The widths and heights of each ring's elliptical air-holes are  $a_1, a_2, a_3$  and  $b_1, b_2, b_3$ , respectively.)

It is already known that the dimension of circular air-holes of some rings close to the central core region greatly influence the dispersion properties of PCF [66]. The same effect

would work when these air holes will be converted into elliptical shape. The circular holes in first three rings starting from center have been modified to elliptical form in their work. The total dispersion comprising of waveguide and material dispersion as well as dispersion slope are visible in Figure 1.15.

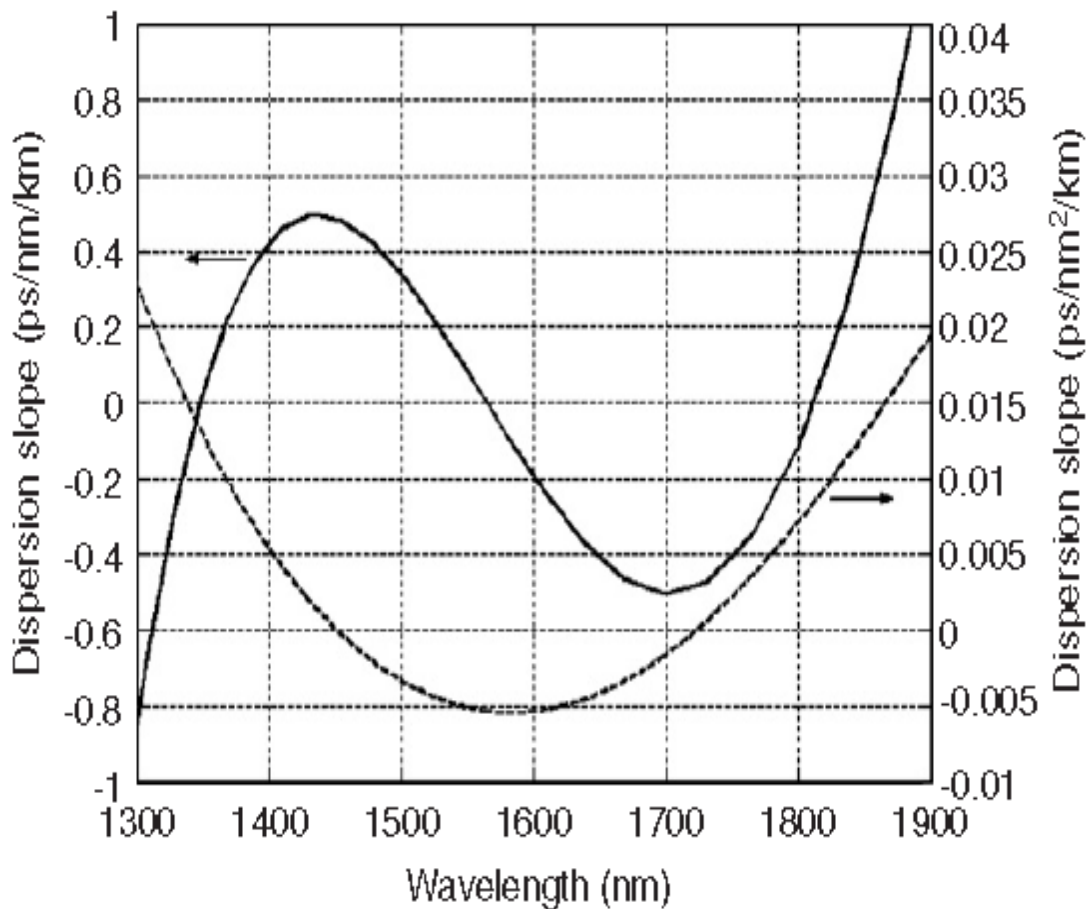


**Figure 1.15** Total dispersion and dispersion slope of modified PCF with  $\Lambda=2.3$ ,  $d=0.908$   $\mu\text{m}$ ,  $a_1=0.7$   $\mu\text{m}$ ,  $a_2=0.723$   $\mu\text{m}$ ,  $a_3=0.71$   $\mu\text{m}$ ,  $b_1=0.55$   $\mu\text{m}$ ,  $b_2=0.55$   $\mu\text{m}$  and  $b_3=0.66$   $\mu\text{m}$ .

Due to the introduction of elliptical air-holes, there takes place degeneracy of the fundamental mode and birefringence comes into the picture. Earlier, many works have

shown birefringence property of PCF arising due to change in dimension of air-holes or asymmetrical core design [67-69]. The birefringence curves for different ellipticity ratios ( $\eta$ ) can be seen in Figure 1.16, where  $a$  and  $b$  denote the minor and major axes of ellipse, respectively.

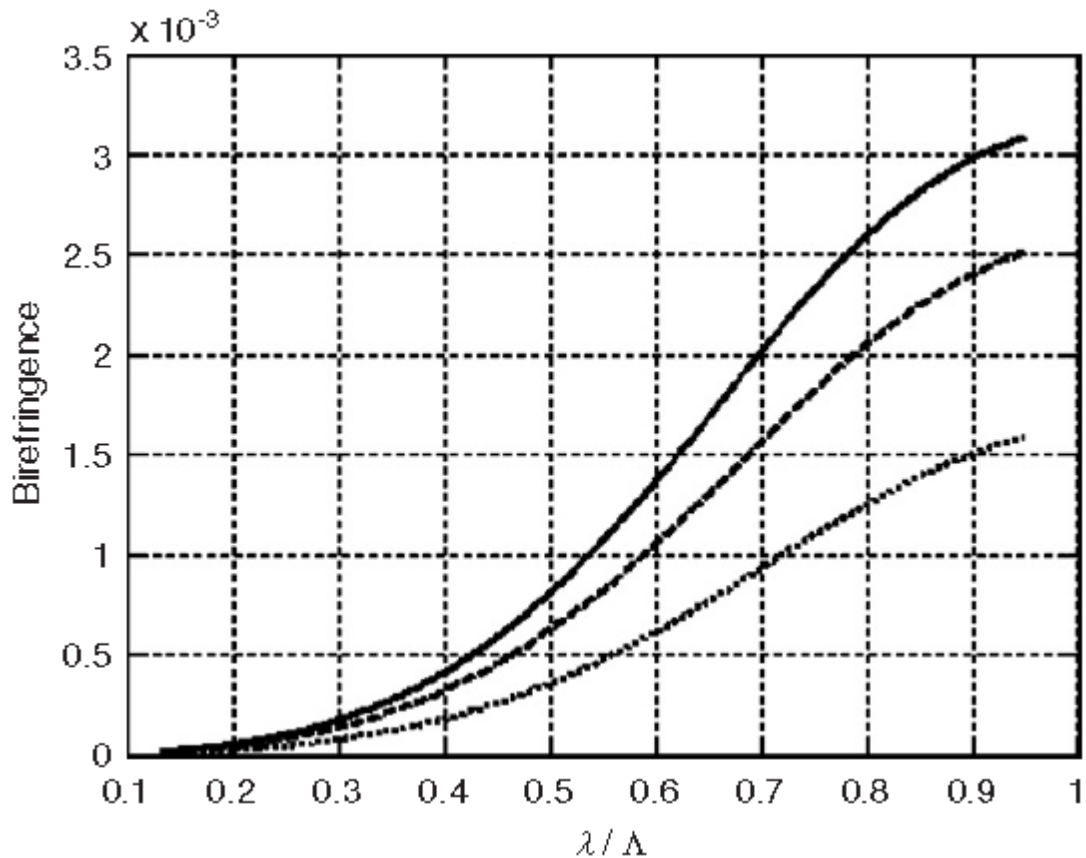


**Figure 1.16** Birefringence  $\Delta n_{\text{eff}}$  of PCFs with  $\Lambda=2.3 \mu\text{m}$ ,  $d=0.736 \mu\text{m}$ ,  $b=2a=1 \text{ mm}$ ,  $\eta=2$  (dotted line);  $b=3a=1.2258 \mu\text{m}$ ,  $\eta=3$  (dashed line);  $b=4a=1.4144 \mu\text{m}$ ,  $\eta=4$  (solid line).

Thus, from their work it can be concluded that both the dispersion and birefringence properties of a PCF can be controlled by converting air holes into elliptical shape and further optimizing their dimension.

A modified form of a rectangular lattice microstructure PCF has been presented by S. Kim et al. in 2009 [70]. They have shown high birefringence and negative dispersion with the help of their proposed PCF. Birefringence is an important property in terms of fiber optics for maintaining the polarization state and reduction of polarization coupling. A plane wave expansion (PWE) method [71, 72] is used to study the properties of modified structure PCF. A rectangular lattice has more anisotropic behavior than the conventional triangular or honey-comb configuration [73]. A schematic of the cross-sections of conventional rectangular lattice and modified rectangular lattice is shown in Figure 1.17.

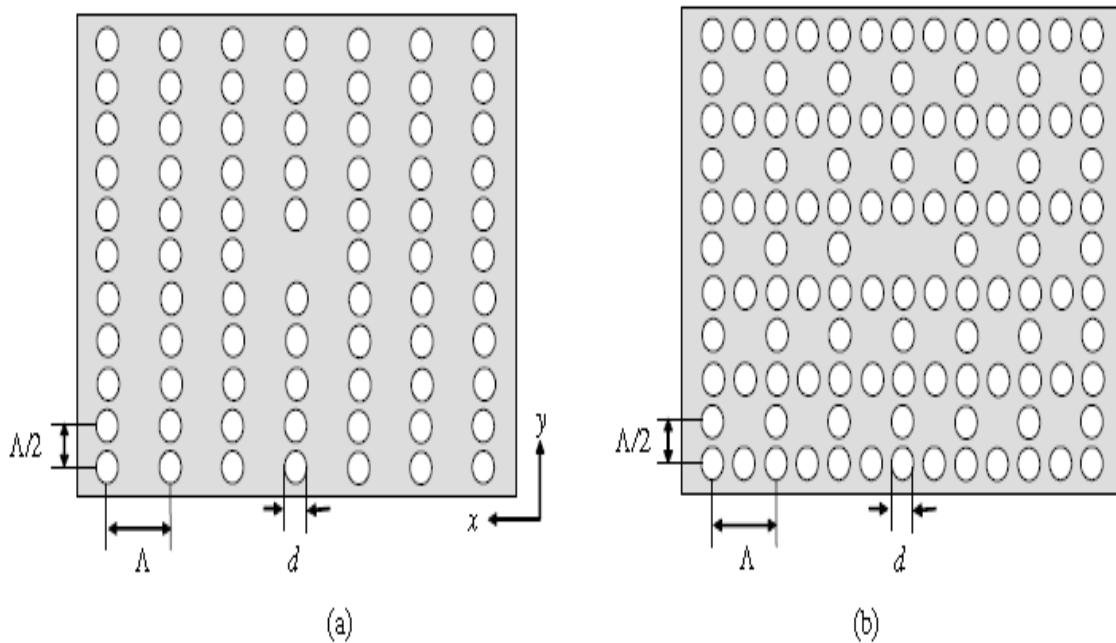


**Figure 1.17** Schematic diagrams of (a) conventional rectangular lattice PCF and (b) the modified rectangular lattice PCF.

As we can see, an extra air-hole is placed in between two air holes in the x-direction to form modified rectangular lattice. This adding of air holes increases the refractive index contrast between core and cladding of fiber, thus leading to high birefringence and better

dispersion compensation. The modal birefringence, leakage loss and dispersion properties of modified rectangular lattice PCF as compared to conventional one can be seen in Figure 1.18 for the lattice parameters  $d/\Lambda=0.4$  and  $\Lambda=2 \mu\text{m}$ . It is observed that there is a huge reduction in the confinement loss of PCF when the geometry is changed to modified rectangular from only rectangular i.e. a shift from  $10^2$  to  $10^{-2}$  dB/m is achieved. A higher negative dispersion slope is seen for the modified rectangular geometry PCF which improves the dispersion compensation ability of PCF. Also, in their work, the values of  $d/\Lambda$  and  $\Lambda$  are varied to see their effect on birefringence and dispersion in and around C-band of communication.

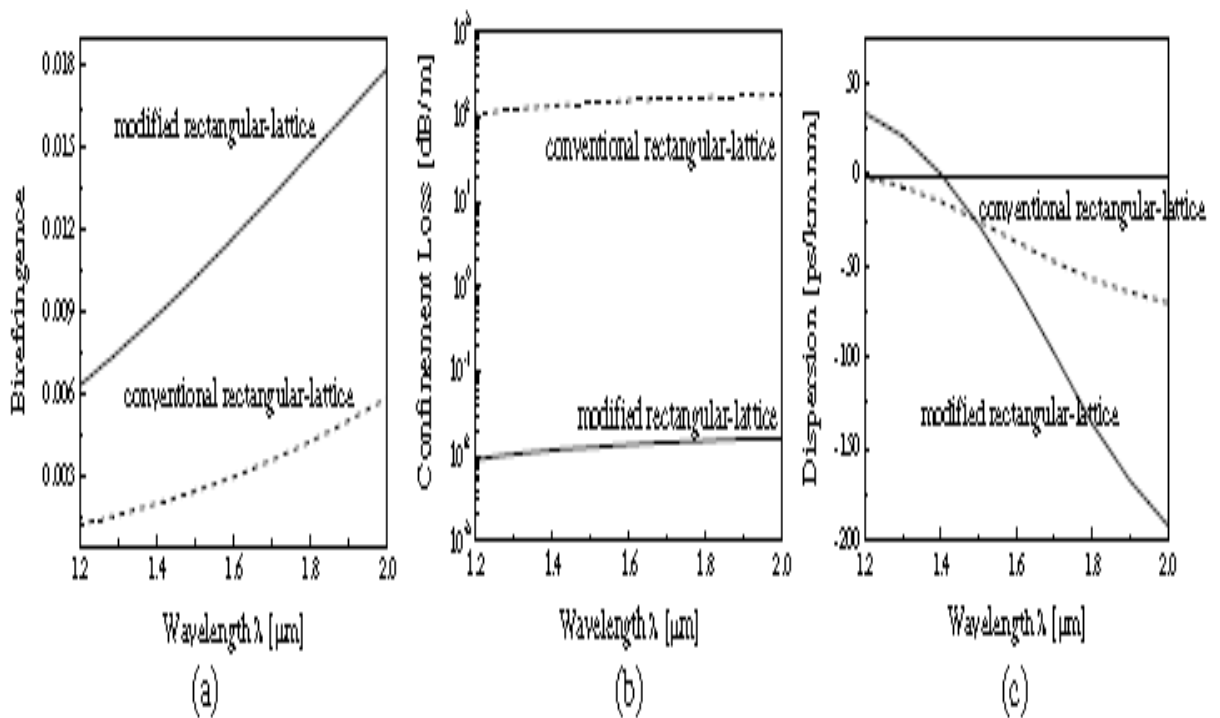


**Figure 1.18** (a) Modal birefringence, (b) leakage loss and (c) chromatic dispersion of the two types of fibers.

M. Chen et al. in 2010 proposed a new design of high negative dispersion photonic crystal fiber [74]. It has a double core structure. In the design of photonic crystal fibers which can compensate chromatic dispersion, there can be used an asymmetrical dual-concentric-core structure for allowing propagation of two super-modes. This dual-core structure is vastly employed in design of the dispersion compensating fibers [75, 76]. A honeycomb lattice PCF has been taken to demonstrate high negative dispersion whose schematic cross-section is visible in Figure 1.19. The cladding contains circular air-holes arranged in a honey-comb array with lattice constant  $\Lambda$ , where  $\Lambda$  is the distance between the centers of two consecutive air-holes. The core region of the fiber is doped with germanium and diameter of air-holes in the first ring has been increased as compared to air-holes present in other rings. The third ring of air holes is eliminated. This structural aspect makes the PCF to couple super mode and generate high negative dispersion [77]. The super-mode generated in the fiber at wavelength 1.55  $\mu\text{m}$  can be seen in Figure 1.20. The inset figure B shows the mode profile propagating in doped core whereas inset figure C shows the mode profile propagating in first ring.

The dispersion curves obtained of the PCF by varying pitch ( $\Lambda$ ) of structure are shown in Figure 1.21. The minimum dispersion obtained is -2300 ps/nm-km at 1.442  $\mu\text{m}$  wavelength and 1.450  $\mu\text{m}$  pitch dimension.

When the diameter of germanium doped core is varied, new types of dispersion curves obtained as visible in Figure 1.22. The minimum dispersion obtained in this case is -1500 ps/nm-km at 1.523  $\mu\text{m}$  keeping diameter of core ( $d_{\text{core}}$ ) equal to 2.00  $\mu\text{m}$ .

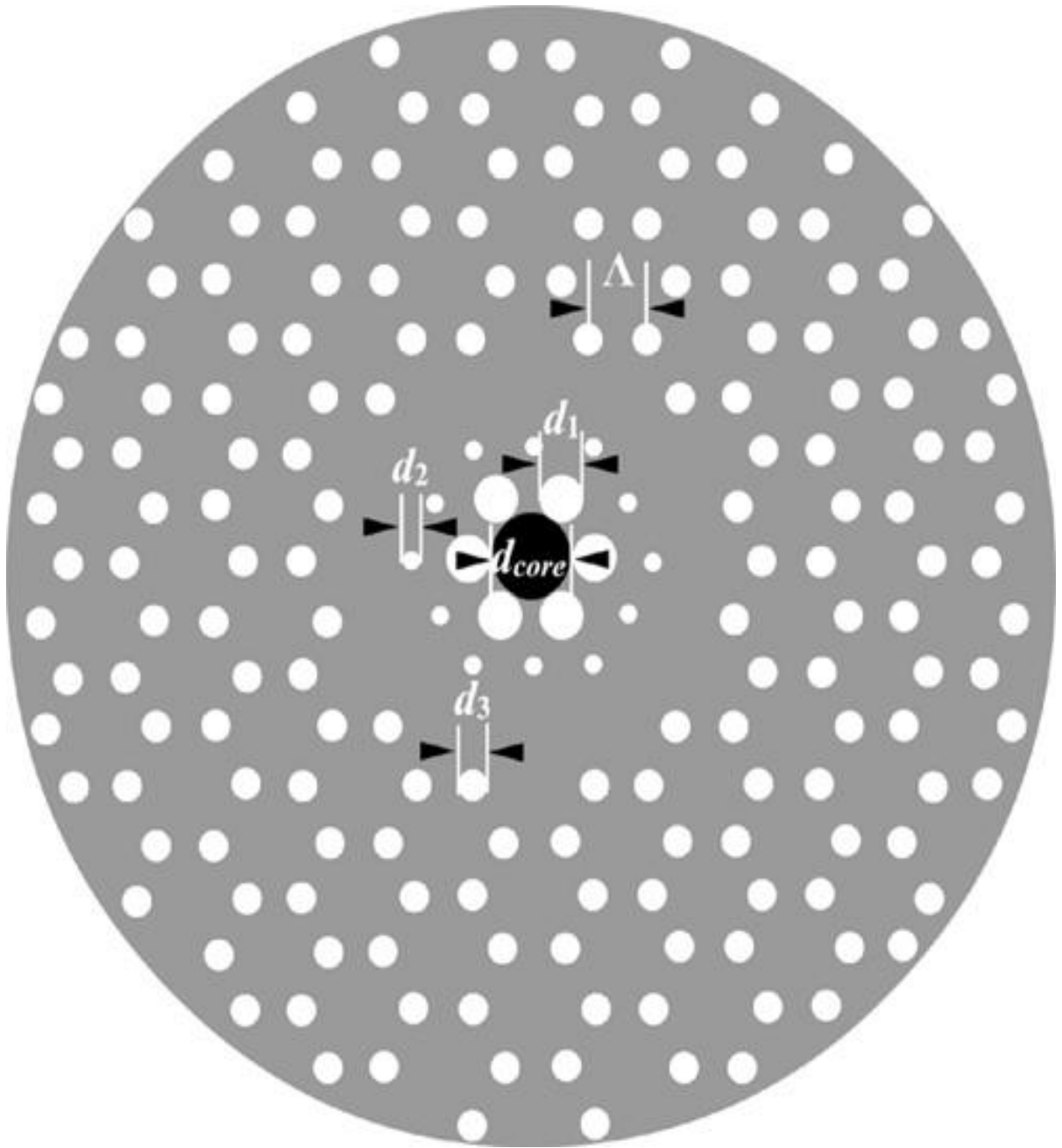


**Figure 1.19** Illustration of the cross structure of the high negative dispersion PCF.

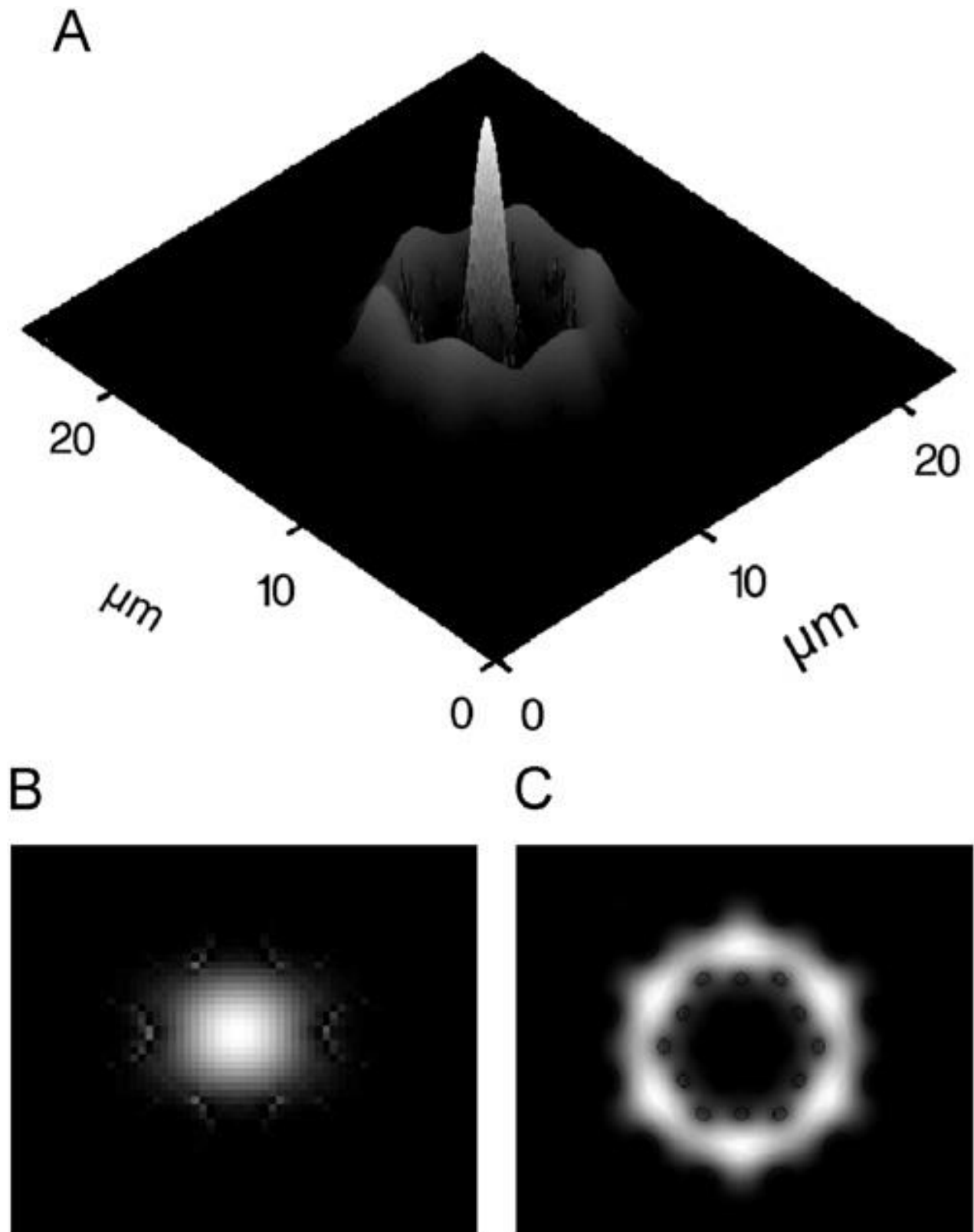


**Figure 1.20** Super mode field profile (A) at 1.55 mm, (B) the core mode profile and (C) the first ring mode profile.

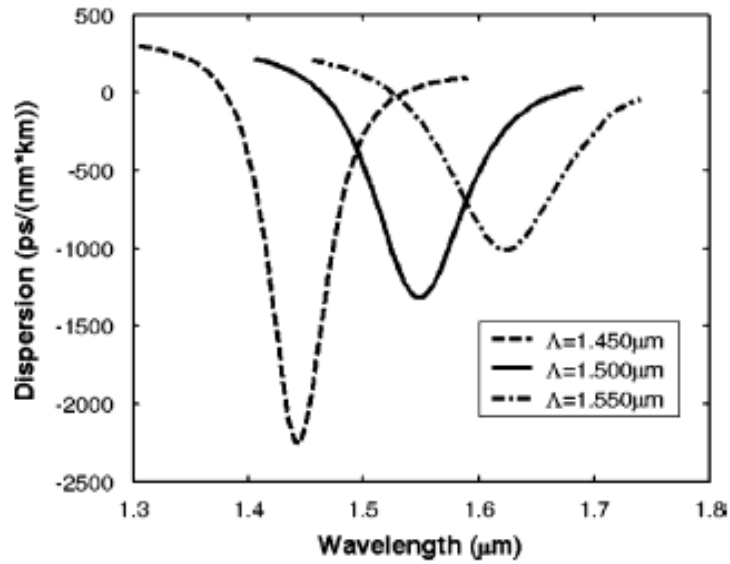


**Figure 1.21** Dispersion curves at different lattice pitch constant viz. 1.450, 1.500 and 1.550  $\mu\text{m}$ .

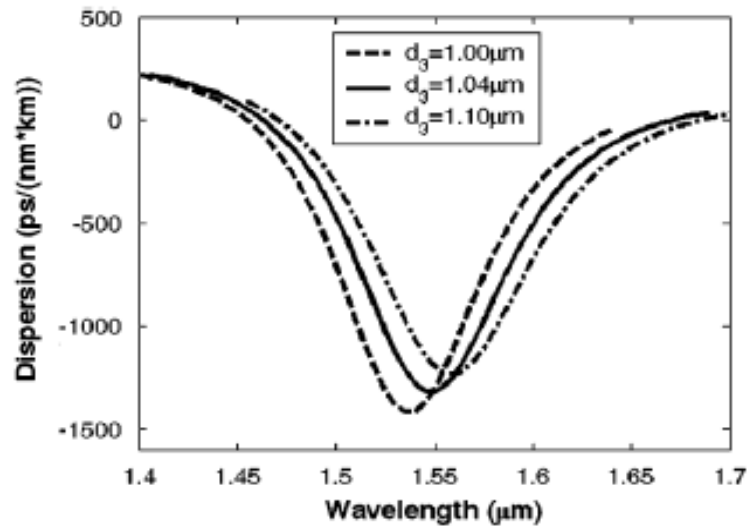


**Figure 1.22** Dispersion curves with different core diameters.

Design of a polarization-maintaining equiangular spiral photonic crystal fiber for residual dispersion compensation over E+S+C+L+U wavelength bands was given by M. A. Islam and M. S. Alam in 2012 [78]. An equiangular spiral photonic crystal fiber (ES-PCF) with smaller effective mode area showing high nonlinearity and ultra-flattened dispersion was reported prior to their work [79]. ES-PCF was also investigated by [80] to generate two zero dispersion wavelengths for the fiber's possible application in super continuum generation within visible region. Talking about the wavelength range E+S+C+L+U, [81] reported a genetic algorithm based optimization technique for achieving a flattened negative dispersion with an average dispersion of -212 ps/nm-km and a dispersion variation of 11 ps/nm-km. Here, an air hole with elliptical shape has been embedded into the core of PCF to achieve a higher and flattened negative dispersion in the combined E+S+C+L+U wavelength band. This structure also displays a very high value of birefringence. Figure 1.23 shows the air hole arrangement in the proposed ES-PCF design with denotation of some air-hole dimensions. The dispersion properties of this structure compared with those obtained in [81] and [82] have been shown in Figure 1.24. A higher negative dispersion is visible with an average of -227 ps/nm-km in the wavelength range 1350-1675 nm. It is also found that the average effective area of this ES-PCF is around  $5\mu\text{m}^2$  and the calculated splice loss is around 6.5 dB. This loss can be reduced using fusion splicing reported in [83]. Further, to make sure the stability of the proposed design, tolerance study was performed by variation of different structure parameters. Total dispersion and birefringence are shown in Figure 1.25 and Figure 1.26, respectively, where the results of the optimized design are compared with the results generated by varying only one parameter at a time. It is observed that a variation of about 5% in the structural dimension makes a minor change in the average dispersion and birefringence. The curves with the dark circle show the results of

the optimized design of fiber, while the other curves show the results with only the parameters varied as shown in the legend.

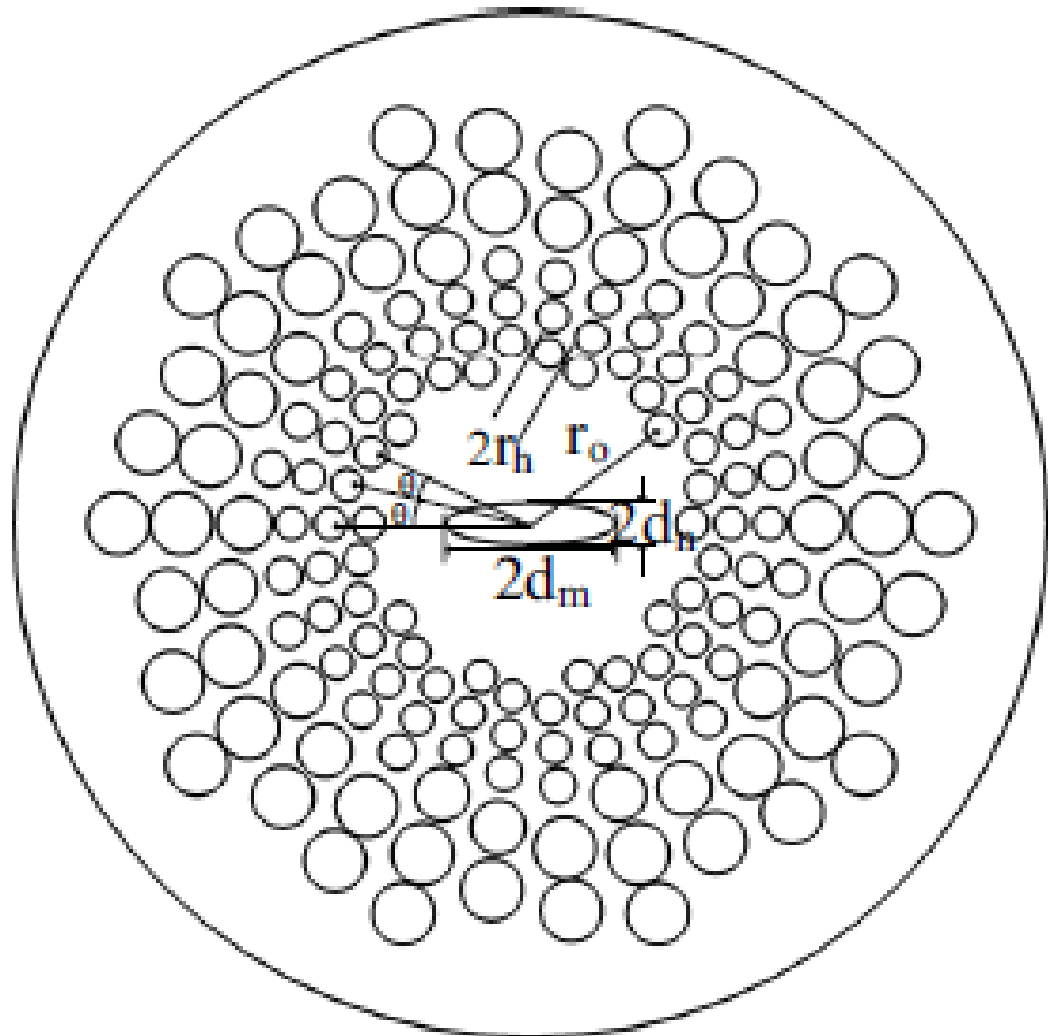


**Figure 1.23** Cross section of the proposed ES-PCF.

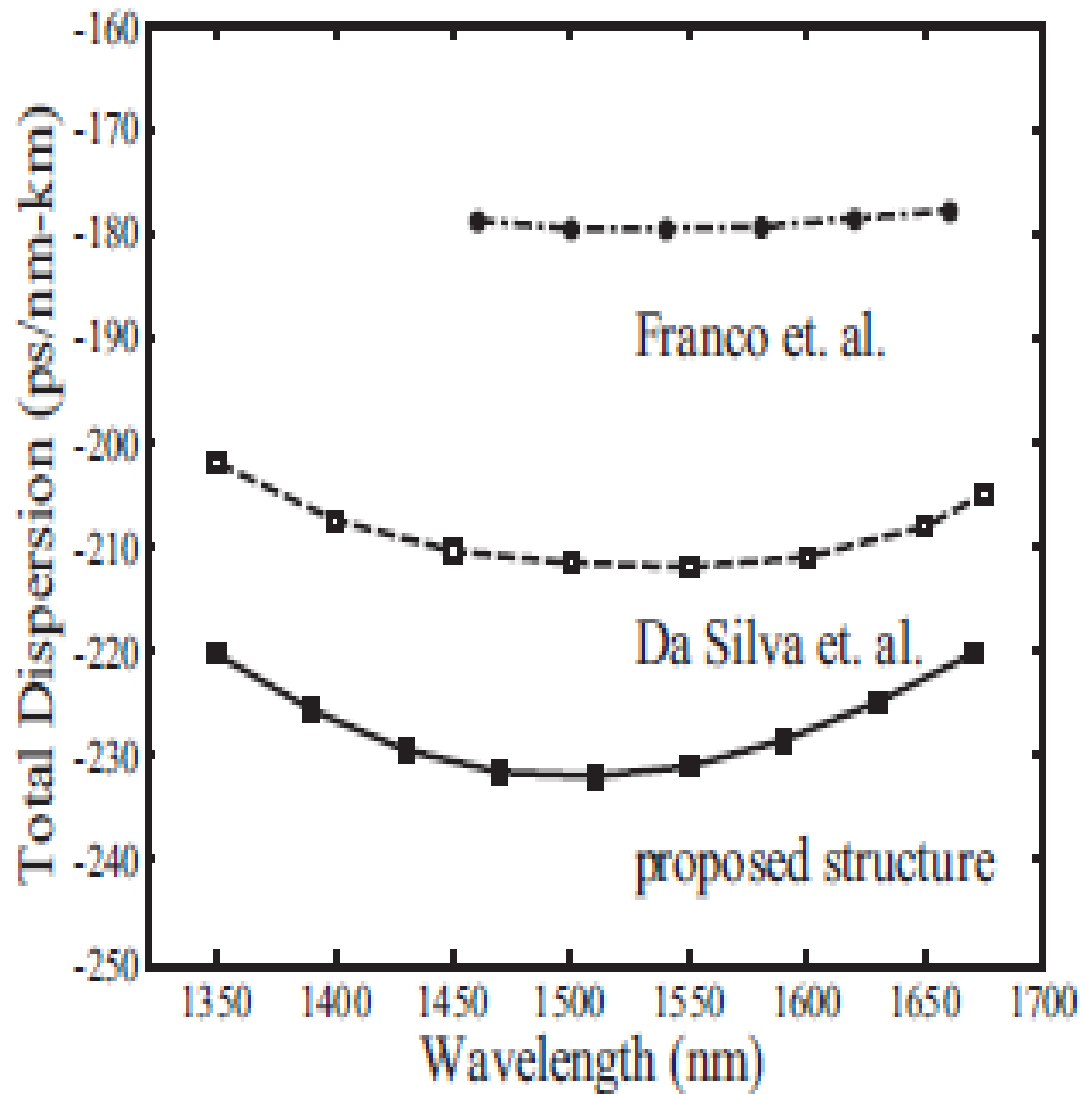


**Figure 1.24** Comparison of the dispersion properties.

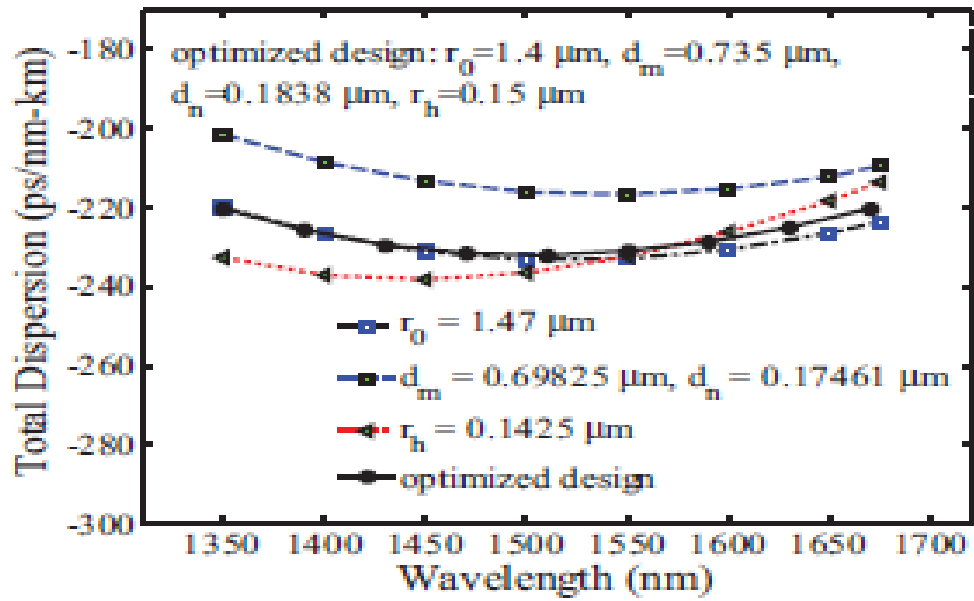


Figure 1.25 Sensitivity of the total dispersion for different structural parameters.

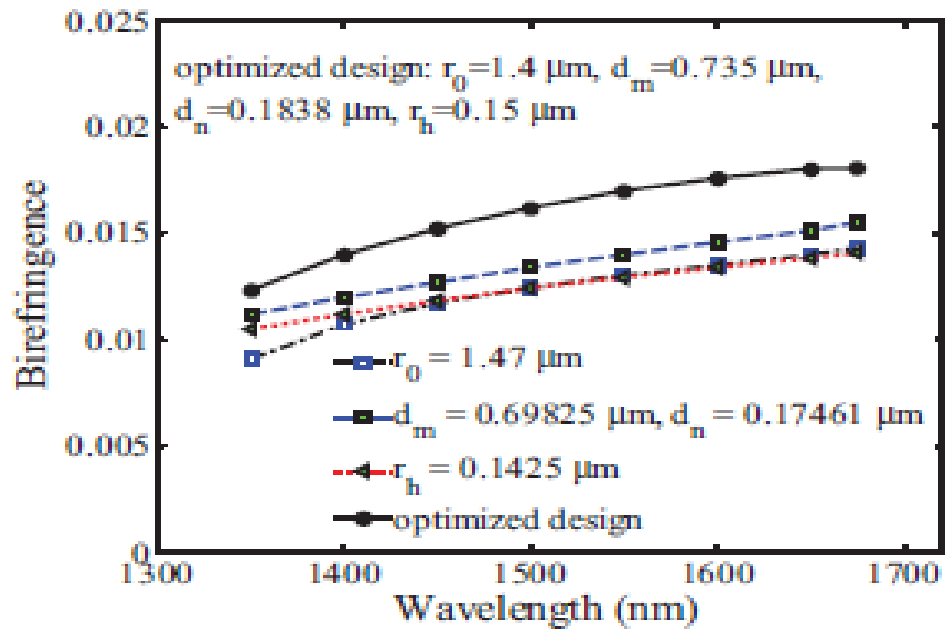
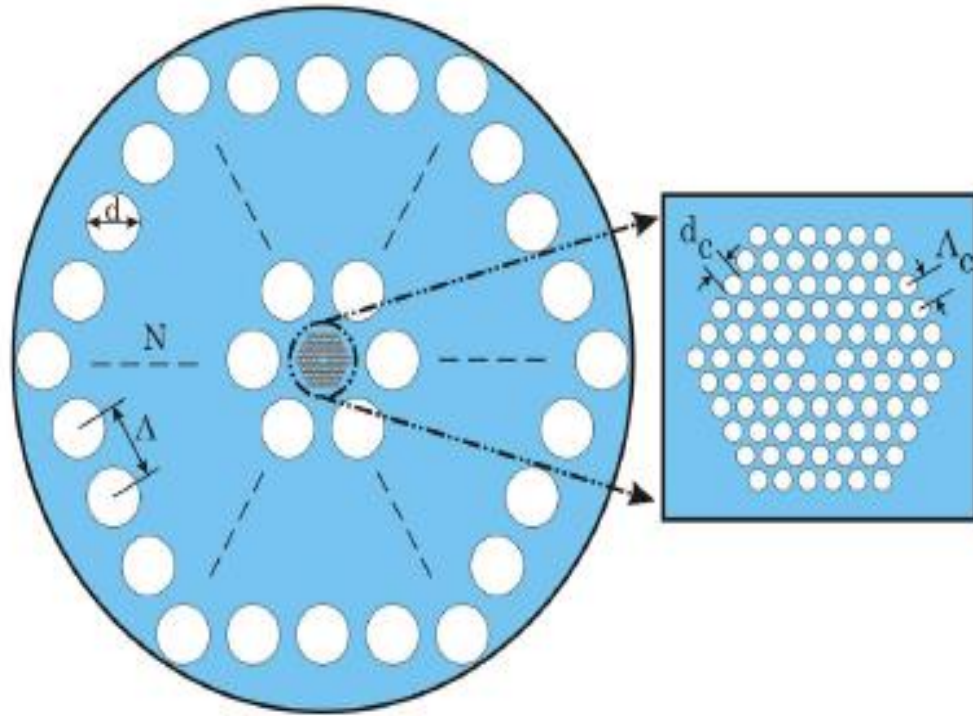


Figure 1.26 Sensitivity of the birefringence for different structural parameters.

Thus, an ES-PCF as a polarization maintaining residual dispersion compensating fiber in the telecommunication frequency bands is investigated. The birefringence value of this ES-PCF is quite high and even higher than most of the polarization maintaining fiber reported earlier.

In long haul optical communications, there is a positive dispersion generated in the conventional optical fibers used for data transmission. This dispersion can be nullified by the application of a dispersion compensating device at a suitable point in the communication architecture. PCFs act as dispersion compensating fibers (DCF) because of their negative dispersion feature to cancel out the positive dispersion of conventional single mode optical fibers used in communication. Even after the application of DCFs, there remains some amount of positive dispersion which needs to be compensated, which is called residual dispersion. D. C. Tee et al. in 2013 [84], presented an innovative design of PCF to solve the problem of residual dispersion. They have proposed a hexagonal lattice PCF-in-PCF structure, as shown in Figure 1.27, able to generate a large amount of negative and flattened dispersion. This type of PCF consists of a hexagonal configuration of air-holes as part of the core and cladding, both of the PCF. This scheme confines light to propagate between the first air-hole ring of the outer lattice and last air-hole ring of the inner lattice PCF. The number of rings containing air-holes in core region is fixed on the basis of achieving high negative dispersion while the number of air-holes in the cladding portion is taken on the criteria of low confinement loss. Software available commercially (Comsol) is used for full-vectorial finite element modelling of PCF.



**Figure 1.27** Transverse cross section of the proposed PCF-in-PCF structure.

By optimizing the parameters of PCF-in-PCF geometry, quite high average negative dispersion is achieved i.e.  $-457.4$  ps/nm-km in E+S+C+L+U communication bands. There is only a variation of  $12.7$  ps/nm-km in the dispersion graph, which makes it more flattened, as visible in Figure 1.28. In this figure  $\Lambda$ ,  $d$  denote the pitch and air-hole diameter of outer hexagonal cladding whereas  $\Lambda_c$ ,  $d_c$  denote the pitch and air-hole diameter of hexagonal structure present in the core of overall PCF. Also, effective mode area and non-linear coefficient have been found out in their work by optimizing of the structural parameters of PCF-in-PCF.

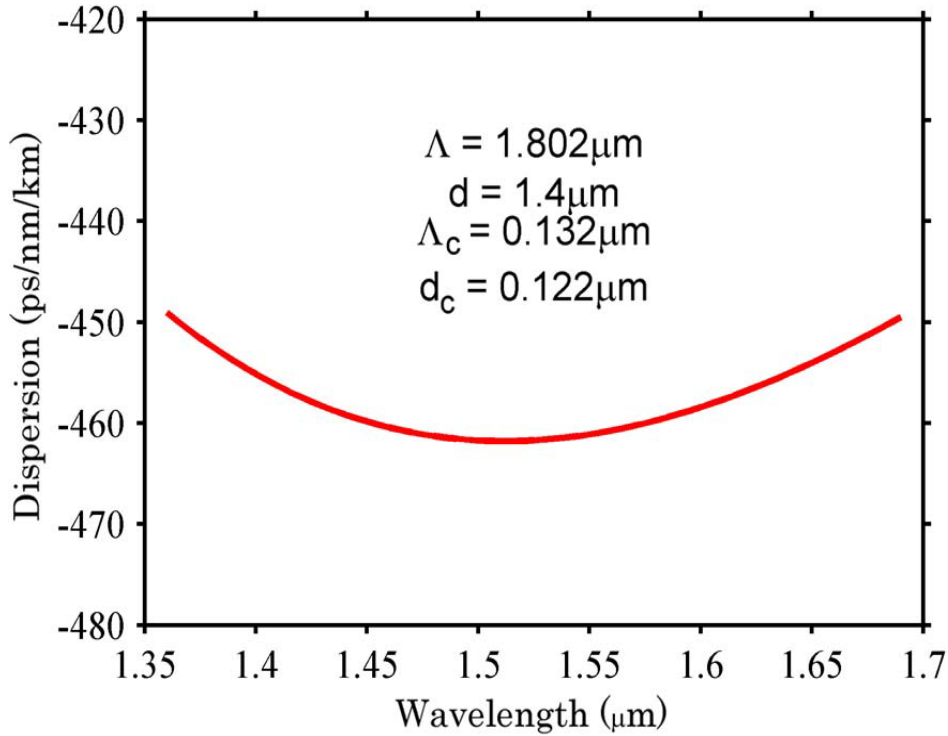


**Figure 1.28** Flattened negative dispersion over E +S +C +L +U wavelength bands at optimum parameters of PCF-in-PCF.

The polarization and dispersion properties of a hybrid PCF design were presented by M. I. Hasan et al. in 2014 [85]. To reduce the insertion loss and decrease the input costs, dispersion compensating fibers (DCFs) need to be smaller in length with ability of compensating higher negative dispersion [86]. Photonic crystal fibers showing high birefringence property are appropriate for various advanced applications which include fast data communication, gyroscope measurement, sensing etc. A number of works have shown high-birefringence PCFs designed by giving an asymmetrical shape to the core of the PCF [87-89]. Here, a simple hybrid PCF structure has been proposed that shows ultra-high birefringence of the order  $3.45 \times 10^{-2}$  and nonlinearity of about  $39 \text{ W}^{-1} \text{ km}^{-1}$  at 1550 nm. A finite difference method (FEM) has been applied to find out the dispersion and other

parameters of the hybrid PCF. Results show that dispersion parameter varies from -356 to -1189 ps/(nm-km) for wavelength in the range 1350 to 1630 nm covering more than E + S + C + L bands of communication. The lateral cross-section of the proposed PCF containing five air-hole rings as part of the cladding is shown in Figure 1.29.

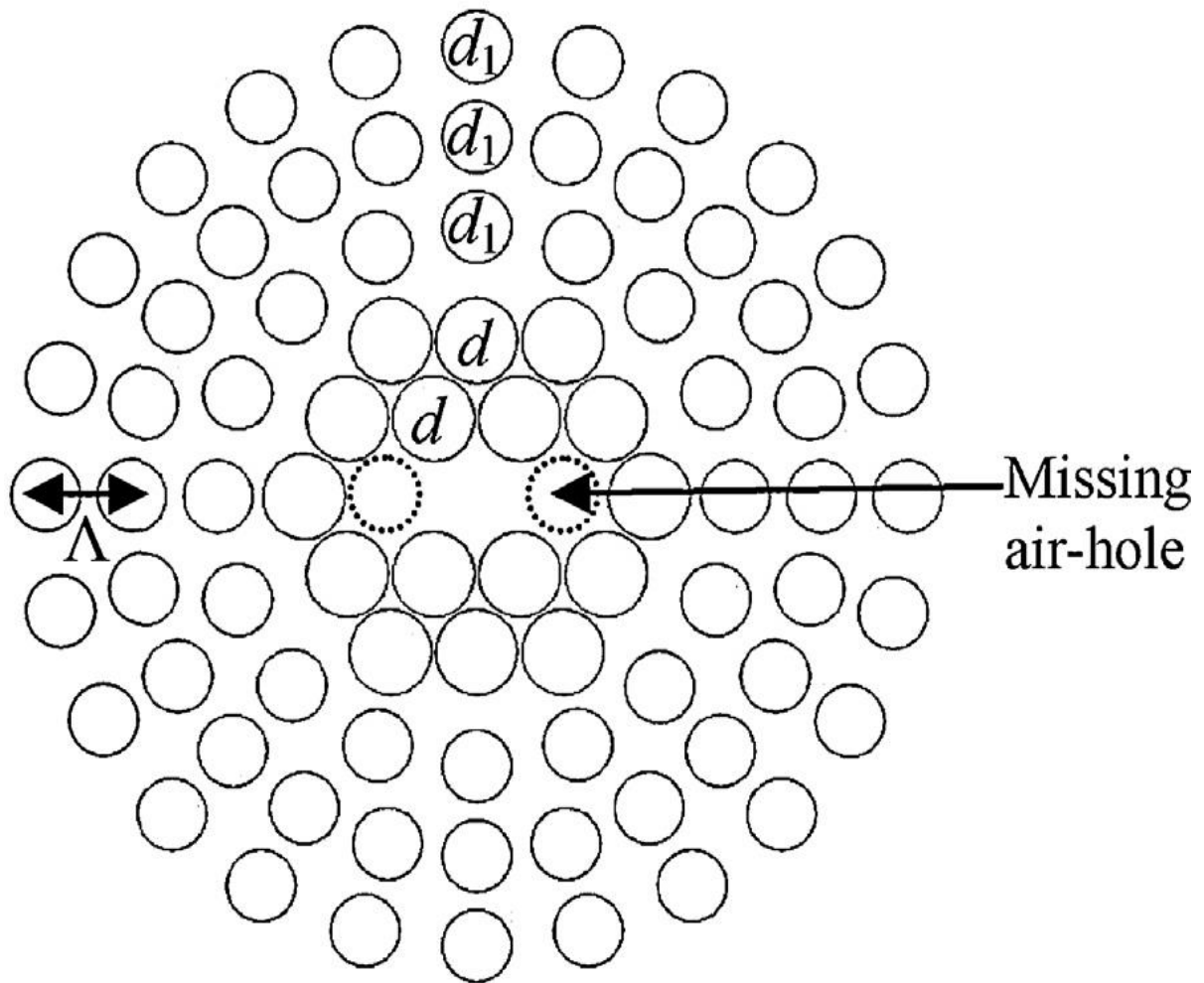


**Figure 1.29** Lateral cross-section of the proposed high birefringence PCF.

Two air holes from the first ring near the core have been removed to form an artificial defect condition. In addition, the first two rings from center have been given a hexagonal shape containing bigger air-holes as compared to other rings which are circular in shape with small air holes. Figure 1.30 shows the dispersion curves of the proposed PCF with small air holes.

optimized parameters  $\Lambda = 0.83$  mm,  $d = 0.8075$  mm,  $d_1 = 0.664$  mm. The designed PCF shows negative dispersion equal to  $-222.25$  ps/nm-km and  $-1054.4$  ps/nm-km at 1550 nm wavelength for x-polarized mode and y-polarized mode, respectively.

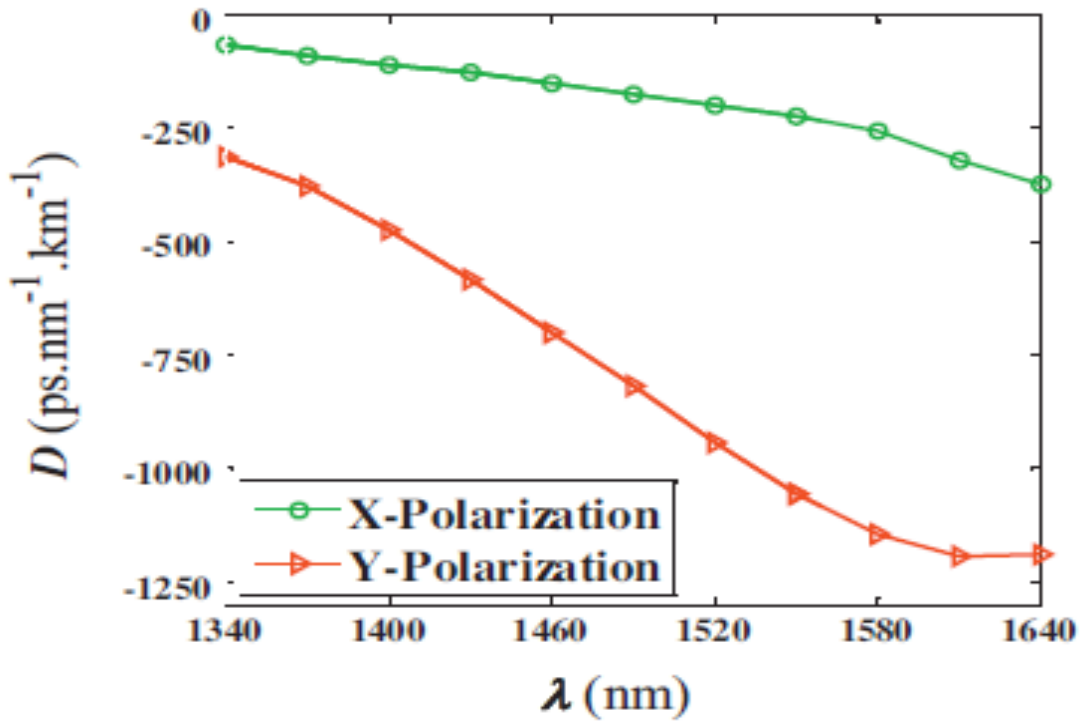


**Figure 1.30** Dispersion properties of the designed PCF for polarization in X and Y direction.

Another figure has been plotted to show the variation in dispersion with change in diameter of holes to pitch ( $d/\Lambda$ ) ratio. Figure 1.31 shows that when the value of  $d/\Lambda$  is increased dispersion parameter on the negative scale also increases at the communication wavelength 1550 nm.

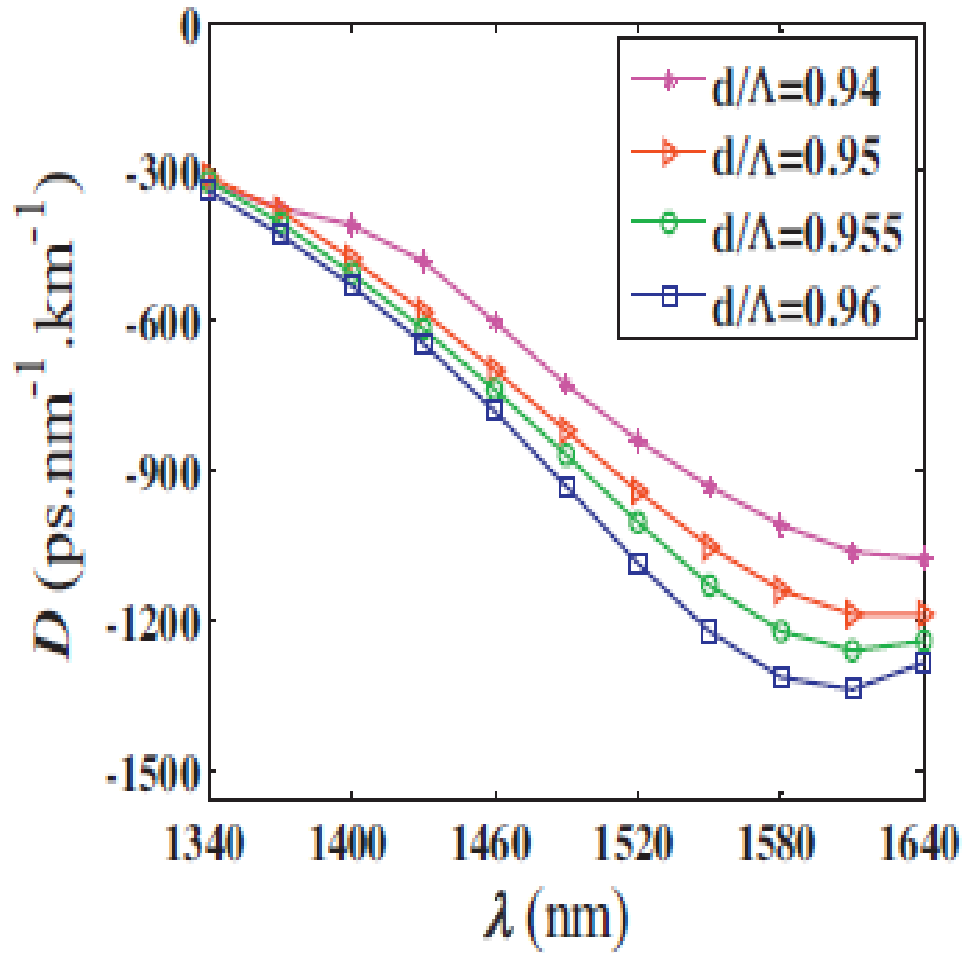


**Figure 1.31** Dispersion properties of the proposed PCF at different values of  $d/\Lambda$ .

The birefringence, nonlinear and normalized frequency characteristics of the PCF are shown in Figure 1.32 and 1.33 respectively.

To conclude, a highly birefringent and highly nonlinear single mode hybrid PCF with artificial defect air-holes in the fiber core and cladding region has been successfully demonstrated based on the FEM method.

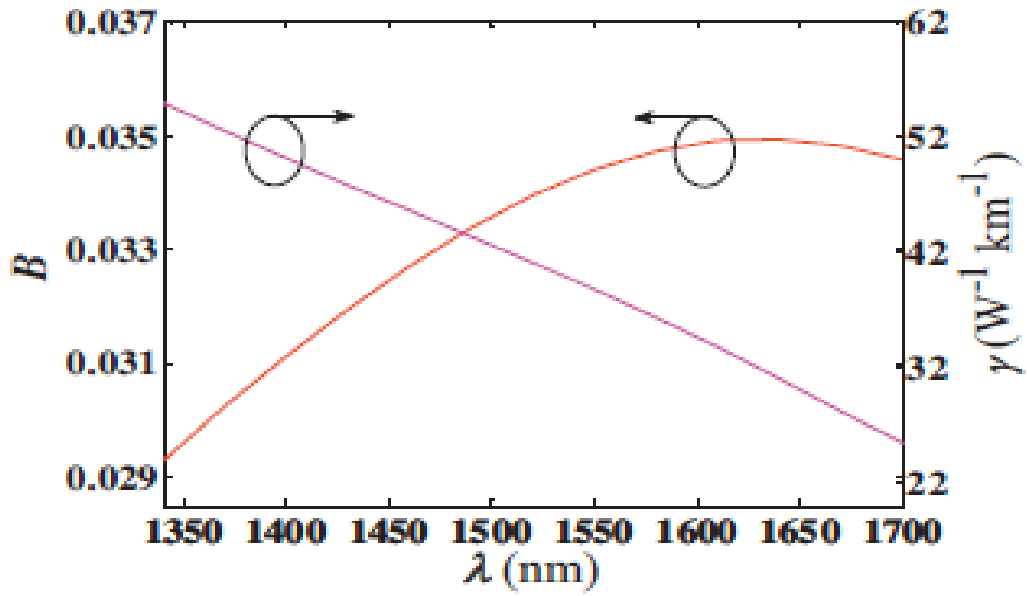


Figure 1.32 Wavelength dependent birefringence and nonlinear properties of the designed PCF.

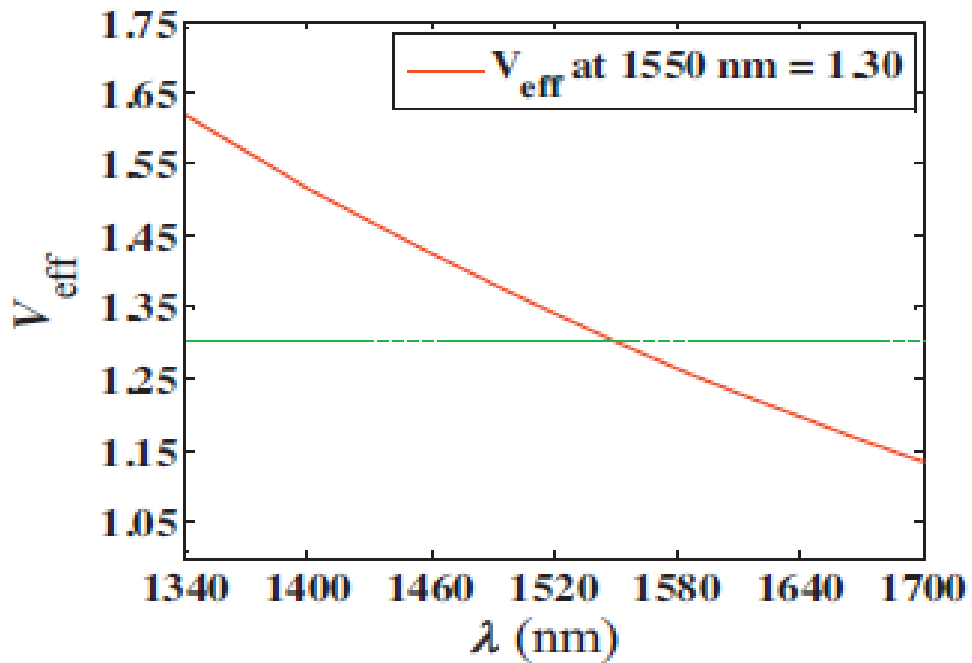
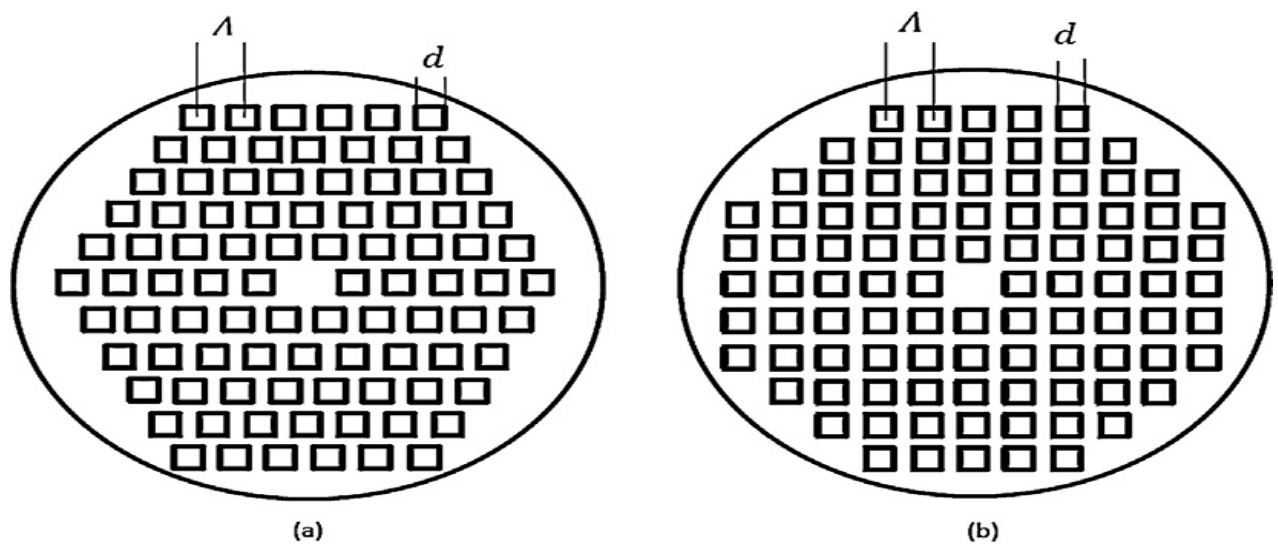


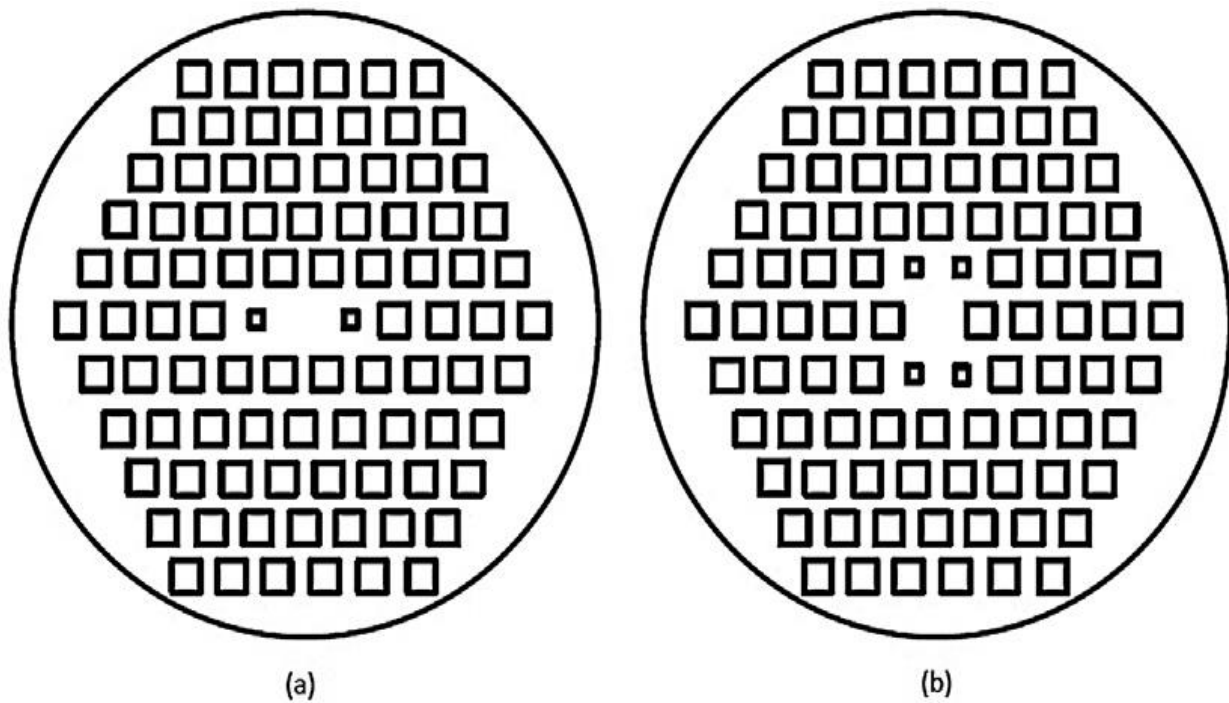
Figure 1.33 Normalized frequency characteristics of the designed PCF.

The shape of the air-holes present in the cladding of PCF can be varied from circular to other types to generate unique properties of PCF. A. Medjouri et al. in 2015 [90] investigated a PCF containing square shaped holes in cladding region for birefringence and dispersion properties. The square holes have been arranged both in triangular and square lattice in their type of PCF as shown in Figure 1.34. A full vectorial FDTD simulation with PML boundary conditions has been applied to the PCF to calculate confinement loss, dispersion and birefringence parameters. The confinement loss is computed to be higher in case of square lattice PCF as compared to triangular lattice one. At the communication wavelength 1550 nm and  $d/\Lambda = 0.53$ , the confinement loss calculated for triangular lattice is close to  $3.5 \times 10^{-4}$  dB/km whereas for square lattice it comes out to be  $2 \times 10^{-2}$  dB/km. To increase the birefringence of square holes PCF two different geometries of PCF were proposed, as can be seen in Figure 1.35. The main reason to design high birefringence producing PCF is to minimize polarization mode dispersion (PMD) in long distance optical communications.



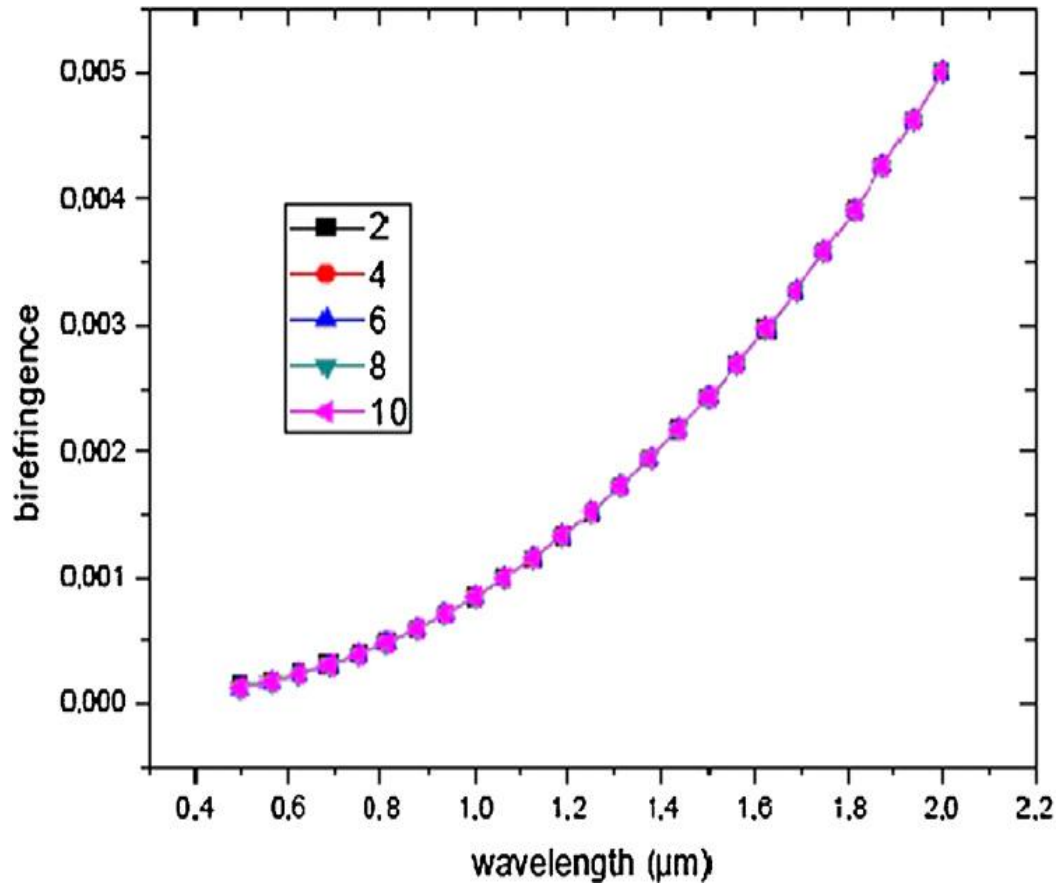
**Figure 1.34** Cross-section of square air holes photonic crystal fiber with (a) triangular lattice and (b) square lattice.

The point to minimize the air holes only in one direction is to generate an asymmetry into PCF which is further linked with fundamental mode eigen-states. As the dimensions of smaller air-holes in any direction are decreased, birefringence gets increased. For improving the chromatic dispersion characteristics, germanium has been doped into the core of the PCF. When the core is doped with germanium in a square region of side  $1\mu\text{m}$ , there is observed a dispersion of  $-260$  and  $-210$  ps/nm-km for the case of triangular and square lattice PCF. Ultra-flattened dispersion curves are generated in case of square lattice PCF containing square holes in the wavelength range  $1$  to  $1.8\mu\text{m}$ .



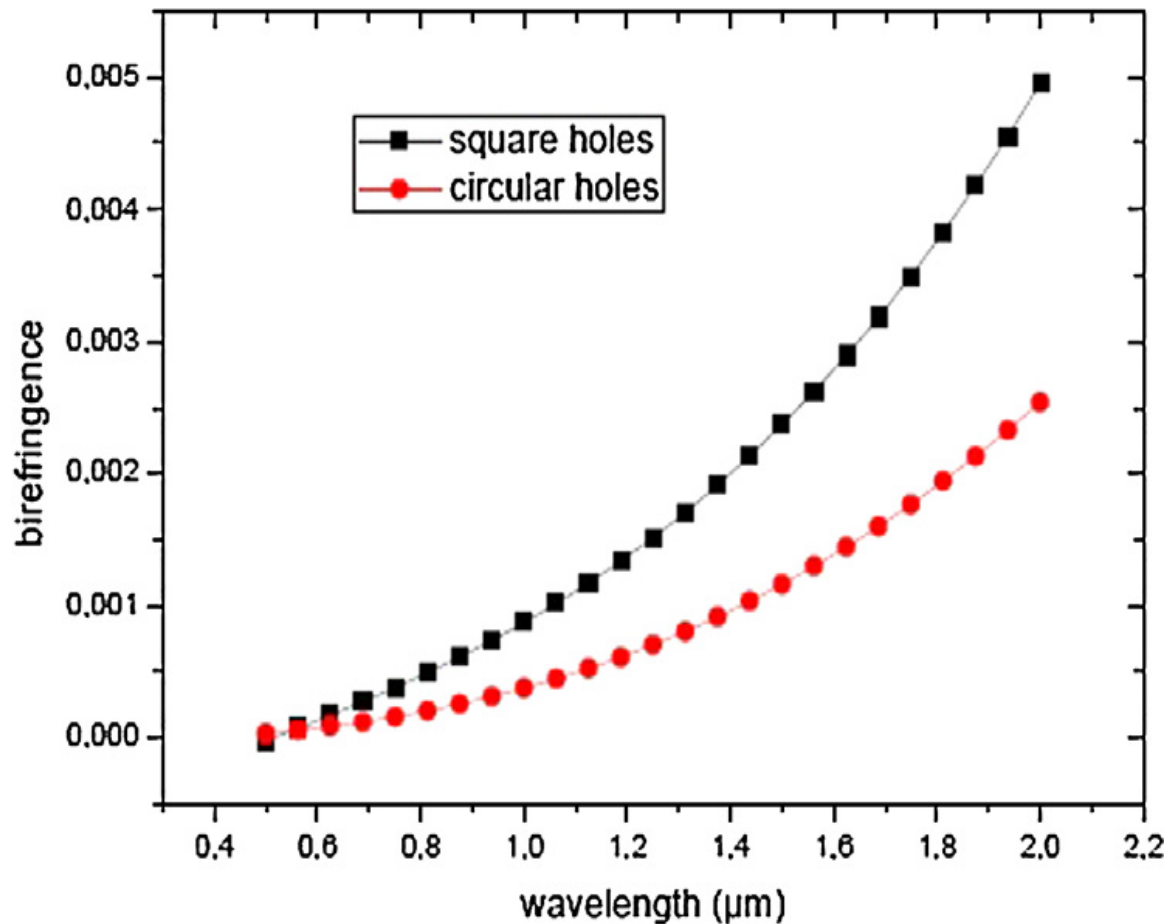
**Figure 1.35** Cross-section of highly birefringent PCF: (a) with two reduced air holes along horizontal axis (b) with four reduced air holes along vertical axis.

Figure 1.36 shows birefringence property as a function of the number of reduced holes in the PCF.



**Figure 1.36** Evolution of birefringence with wavelength for different number of reduced air holes.

Figure 1.37 shows birefringence property as a function of the number of reduced holes in case of square and circular holes based PCF.



**Figure 1.37** Evolution of birefringence with wavelength for PCF with square and circular air holes.

### 1.5 PHOTONIC CRYSTAL RING RESONATOR (PCRR)

PCRR is derived from the class of optical ring resonators in which there are two channel waveguides and a central ring cavity. PCRR can be formed by removing a specific number of dielectric rods in particular shapes from a 2-D PC structure as shown in Figure 1.38 [91]. The rods which connect cavity region of the structure to the channel waveguides are known as coupling rods. One has a flexibility to modify the refractive index and/or radius of the rods present in the cavity and coupling rods both. This modification leads to

shift in the output resonant frequency from the PCRR. At resonant condition in PCRR, there occurs phase as well as frequency matching between the proliferating mode in waveguide and that in cavity region. Optical devices such as power-splitter [92], biochemical sensor [93], add-drop filter [94], de-multiplexers [95] etc. can be built based on PCRR. A photonic device based on the PCRR structure can specially be utilized in the medicine industry for testing of different types of chemicals.

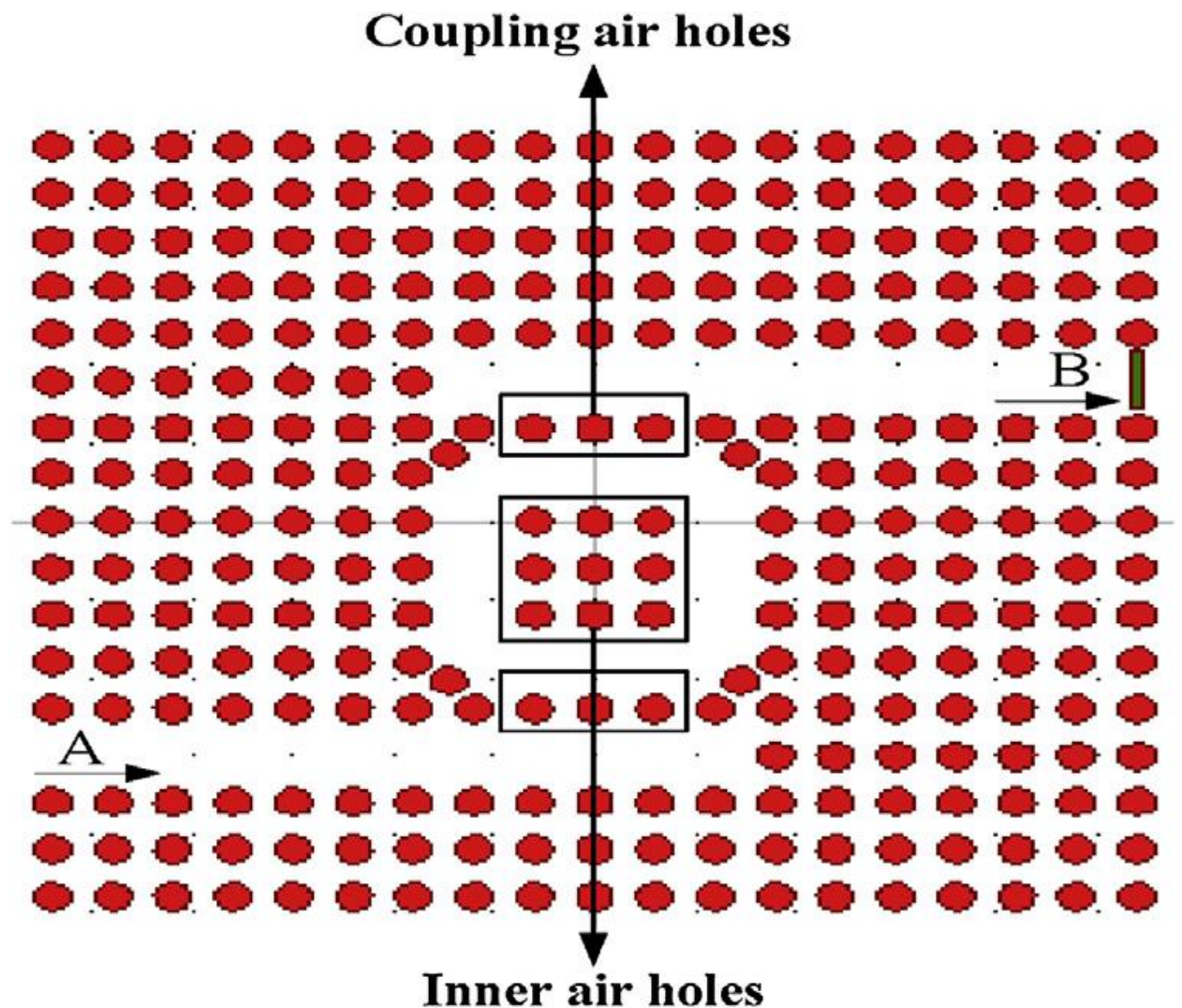


**Figure 1.38** Layout sketch of the PCs based ring resonator structure.

Theoretical investigation of ring resonators in photonic crystal circuits was done by V. D. Kumar et. al in 2004 [96]. They had created rings of rectangular shape in square lattice 2-D photonic crystals. Finite difference time domain method was used to determine the transmission characteristics of the ring resonator structures. A number of dips in the transmission spectrum were observed in case of ring embedded structure whereas the transmission is smooth in case of without ring structure. At the sharp corners of the rectangular ring, an extra photonic crystal rod was placed so that the dip in transmission gets decreased. Also, the interaction distance between the channel waveguide and the ring was decreased by them, and its effect was seen on the transmission characteristics. They studied that three parameters are responsible for variation in resonant frequency of ring resonator viz. ring dimension, refractive index and filling ratio of rods.

Optical add-drop filters (ADF) are a key component of photonic integrated circuits (PICs) and have major applications in optical communication systems. Photonic crystal ring resonators as optical add-drop filters were studied by Z. Qiang et. al in 2007 [97]. They had designed a square ring photonic crystal (PC) structure and simulated it using a 2-D finite difference time domain technique. The refractive index of dielectric rods is fixed at 3.59 in the PC structure, these rods are placed in air medium with refractive index as unity. Initially, they plotted photonic bandgap and dispersion of a line waveguide created in PC structure. A broadband wavelength range 1270 to 1740 nm is found to guide only a single mode for the line defect waveguide. In case of square ring photonic configuration, scattering rods have been placed at the corners of the ring with equal radius as the other rods of 2-D structure. These scattering rods provide the advantage of accuracy in spectral extraction and provide a high efficiency of the dropping waveguide at the resonant

frequency. Although, the value of quality factor ‘Q’ was achieved only as 160 in the case of single ring PCRR. To further improve the spectral selectivity and Q value, dual ring PCRR was proposed, as shown in Figure 1.39.

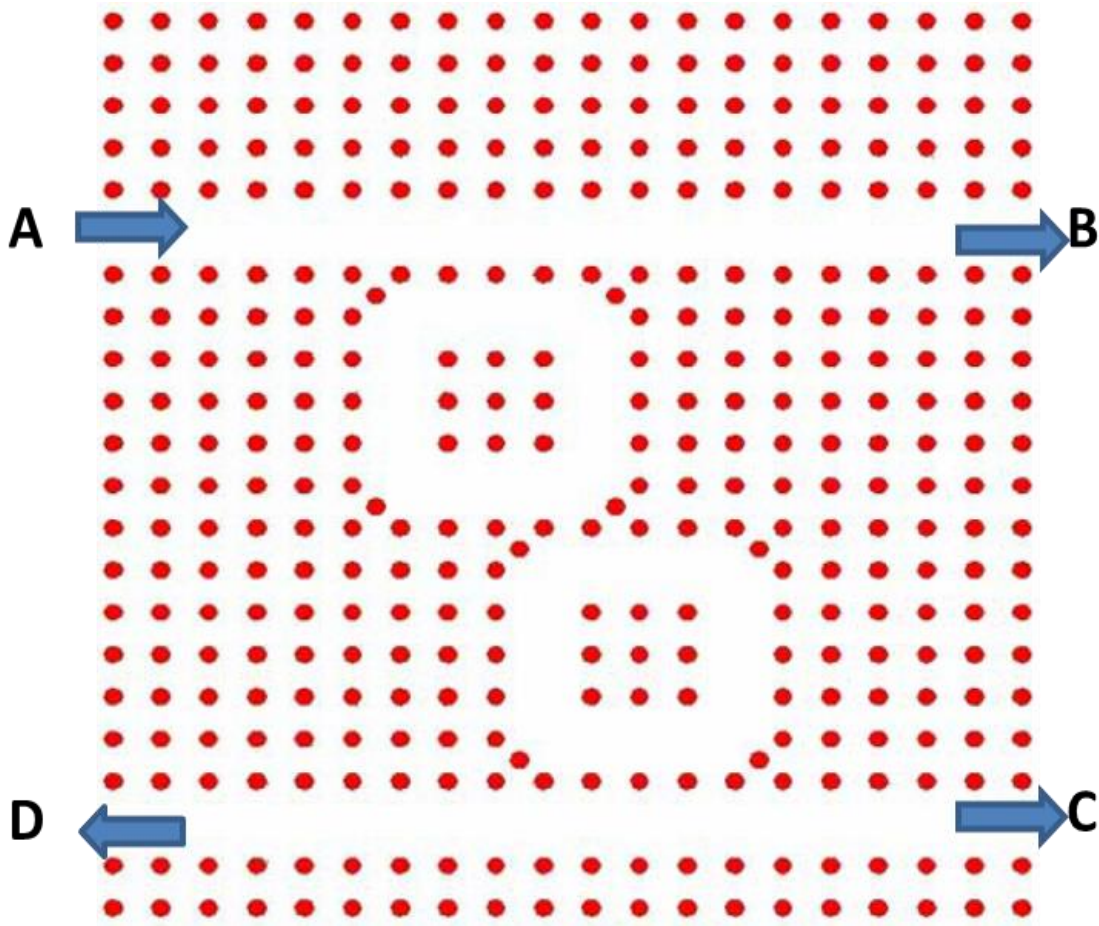


**Figure 1.39** Schematic of dual-ring PCRR based ADF for backward-dropping due to weak coupling between two rings.

In this case, two types dual ring PCRR were studied, one with backward dropping feature and the other with forward dropping quality. The backward dropping PCRR contains coupling period between two rings as  $2a$ , while the forward dropping PCRR consists of  $4a$  as the coupling period. The parameter ‘a’ stands for lattice constant in the PC structure, a distance between two consecutive photonic crystal rods. The resonant coupling

in PCRR occurs due to the frequency and phase matching of the propagating mode and resonant mode in the cavity. The coupling configuration can decide whether there will be a forward dropping or backward dropping of resonant wavelength. Optical switches and rearrangeable wavelength division multiplexers can be achieved based on the proposed one and two ring PCRRs.

Power splitters based on Y-shape or T-shapes have been studied and theoretically investigated in many of the works [98, 99]. The Y-junction splitter is mostly implemented on air holes triangular lattice arrangement while T-junction is realized in silica rods square lattice structure. A. Ghaffari et al. studied and numerically investigated an L-shaped bend and T-shaped power splitter based on PCRR in their work in 2008 [92]. The refractive index of dielectric rods is taken to be 3.46 and surrounding medium as air with refractive index unity. The distance between two consecutive rods, also known as lattice constant ( $a$ ) is fixed at 540 nm and the ratio of rod's radius to lattice constant is set as 0.185. An extra scattering rod has been placed at the bend points of L-shape as well as square ring. These scattering rods help to vanish the back-reflections which cause noise output in the spectral characteristics. A coupled mode theory (CMT) [100] has been used to investigate the interaction between ring cavity and L-shape waveguide. After the L-shape, T-shape waveguide is designed into the PC structure. This waveguide has two ring cavities placed adjacent to its bends so that there is better efficiency and selectivity achieved at the outputs as compared to the conventional T-shape structure. Figure 1.40 shows a schematic of the proposed T-shape waveguide and its transmission characteristics calculated with the help of FDTD.

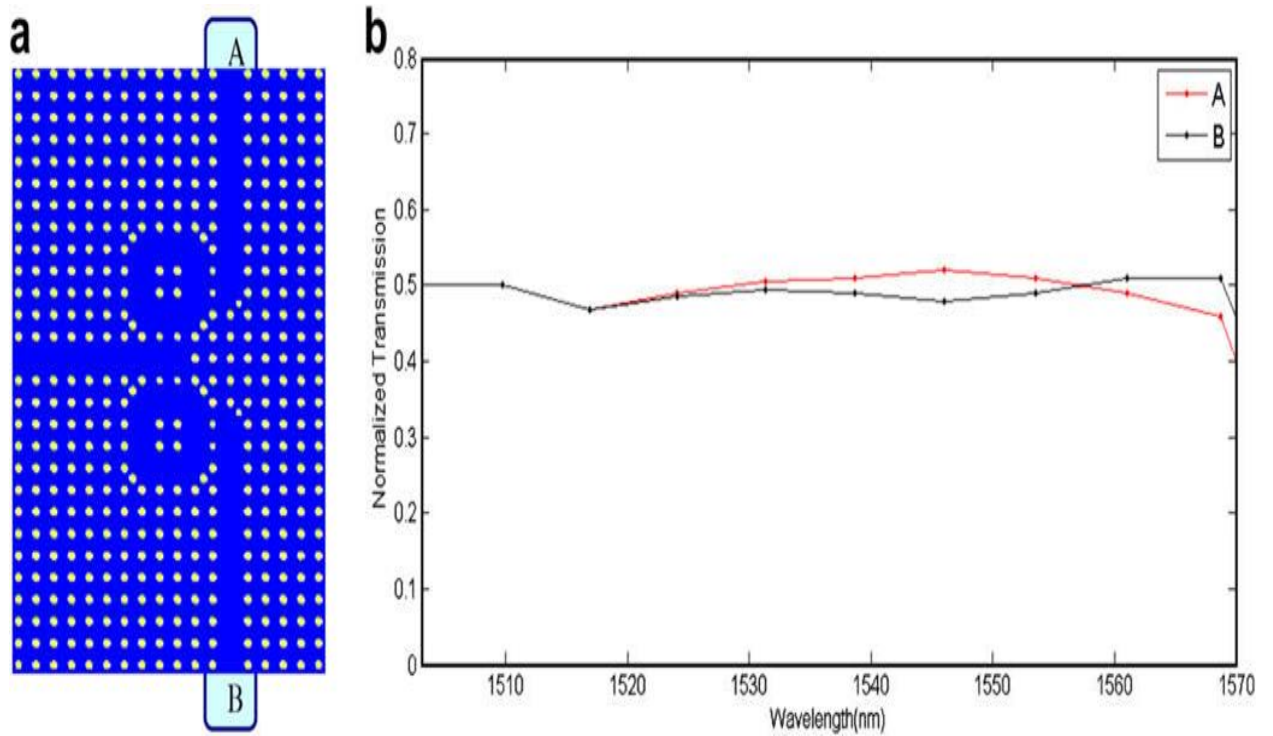


**Figure 1.40** (a) T-shaped power splitter containing 2 ring resonators (b) Normalized transmission spectra evaluated at two output ports.

The ring sizes are optimized by modifying the number of rods situated in the ring for better output efficiency and adjusting of output bandwidth.

Photonic crystal structures can be applied to form all-optical logic gates which have their further application in photonic circuits [101, 102]. Optical fibers can also be used to realize optical gates [103] but PC based gates are faster to implement, have small size and consume less power. Several works have been done to accomplish optical gates using the PCRRs [104, 105]. J. Bai et al. in their work in 2009 studied NOT and NOR logic gates built from a PCRR containing silica rods [106]. They tilted the angle of PCRR to 45 degree and fixed the refractive index of dielectric rods of the whole PC structure as 3.48. There are two input ports attached to the structure alongwith one probe port and one output port. The

gating works on providing simultaneous inputs to two input ports for realizing NOR gate and giving input signal one at a time for NOT gate.

PC structure based bio-chemical sensors have gained a lot of interest due to the small dimension of sensor and high sensitivity. Also, samples of the order of nanometers can be applied to the PC structures using direct-write dip-pen nanolithography (DPN) [107]. F. L. Hsiao and C. Lee in their work in 2011 have proposed bio-chemical sensors based on PC structure containing ring cavity and waveguide. Holes are crafted upon silicon substrate in a hexagonal lattice arrangement. Two types of PC structures are formed, one with a single hexagonal ring and other with two hexagonal rings. The rings are formed by filling up air-holes with that of the background material silicon in a hexagonal manner. Two types of methods have been used to simulate the PC structures viz. effective refractive index and FDTD [109, 110]. The distance between two nearby holes is fixed at 410 nm whereas the radius of holes is taken to be 120 nm in case of single ring cavity and 145 nm for double ring cavity. This type of sensor offers more versatility in sensing as compared to the sensors which are capable of detecting only a single chemical. Also, this type of sensor works in a real-time environment.

## **1.6 MOTIVATION**

PCFs have important application in optical communications. They are used as dispersion compensation devices in long distance optical communications. There is a lot of scope in research based on PCFs by either modifying its structural parameters or manufacturing it from different materials. Bio-sensors based on photonic crystals have compact size, low cost of operations and are convenient to use. There can be done real-time

monitoring of the signals generated through samples in PC based sensors. PCRR based on PC structure acts as a specialized sensor for sensing of bio-chemicals in a rapid and productive fashion.

In the present study, PCRR simulation is done based on circular ring and square ring PC structures for application in the bio-sensing regime. Finite-difference time domain technique with perfectly matching layers (PMLs) is applied to calculate the transmission characteristics of the proposed sensor. Nano photonic device based on our ring resonator structure can act as a potential candidate to serve in industrial or research sector which are working in the field of medicines, food testing, defence etc.

PCFs based on hexagonal and square lattice structures have been studied in this research. The air-holes shape has also been varied from circular to square in one of our work. In case of a square lattice PCF with square air-holes high dispersion tolerance, flattened dispersion and low effective mode area have been achieved. Metals whose dielectric function follows Drude-Lorentz model have been inserted into the air-holes of a square lattice PCF with circular holes. The effect of temperature on dispersion compensation characteristics is studied for a hexagonal PCF.

## **1.7 ORGANIZATION OF THESIS**

The existing thesis has been divided into 7 chapters. Chapter 1 gives an introduction of photonics along with photonic crystals and its two major applications i.e. PCF and PCRR. In the same chapter literature review of PCFs as well as PCRR has been provided. Chapter 2 discusses the variation of refractive index on the dispersion characteristics of a hexagonal lattice PCF. Effect of dispersive materials on the dispersion and normalized frequency

characteristics of a square PCF is analyzed in Chapter 3. Chapter 4 presents the effect of temperature on the dispersion characteristics of a hexagonal PCF. Chapter 5 presents a photonic crystal fiber containing square holes in a square lattice showing high dispersion tolerance, flattened dispersion and low effective mode area. The construction and applications of a highly sensitive bio-chemical sensor based on PCRR is presented in Chapter 6. The conclusions drawn out of the existing research and the future extent of works are outlined in Chapter 7.